

May 18, 2015

MASTER THESIS

MEASUREMENT OF NETWORK ACTIVITY IN ACUTE SLICES OF THE HEALTHY AND PARKINSONIAN STRIATUM ON MICROELECTRODE ARRAYS

FREDDY GUNNEWEG

**Faculty of Electrical Engineering, Mathematics and Computer Science (EEMCS)
Biomedical Signals and Systems (BSS)**

Exam committee:
prof.dr. R.J.A. van Wezel
dr.ir. Y. Zhao
dr.ir. T. Heida
dr.ir. J. le Feber
prof.dr J.C.T. Eijkel (BIOS)

Documentnumber
Electrical Engineering — BSS 15-10

UNIVERSITY OF TWENTE.

Acknowledgements

Before you lays the result of the last 9 months of work I have put into the understanding of the brain in Parkinsons disease. This project is the last achievement required to obtain my masters degree at the University of Twente, and hopefully gives the reader a good overview of my accomplishments and insights. Although the original goals of this project (i.e. measuring network effects of fast spiking interneurons in the striatum) could not be measured, this project has provided new insights in how to appropriately measure neuronal activity in the silent striatum, and may give new deliberations regarding work on acute slices of the basal ganglia.

I came to the BSS lab as a student in Electrical Engineering but with a great interest in neurophysiology and signal processing. I found that the work previously done by my supervisors was intriguing and this project gave me an opportunity to further extend my insights into neuroscience and to delve into a research field that was almost completely new to me.

This process has been a very interesting, engaging, at times frustrating but ultimately very instructive experience that has given me many new insights into both the theory and neuroscience, which is still very much in development and despite experiences in internship and courses also still very mysterious. I have had the opportunity to come up with my own ideas for a research proposal. Although Ive had to significantly alter my original proposal when experiments did not succeed, it was a fruitful experience to be more independent in my research.

I would like to thank my committee for help and guiding me in this project; Yan Zhao, Richard van Wezel, Ciska Heida, Joost le Feber and Jan Eijkel have each given me essential feedback on whether I was on the right track. Although we have had few times to discuss with each other, they have continuously tried to refocus my work, especially when I was less satisfied with my work than they were. Yet they also gave me sufficient opportunities to choose my own methods and process. This has sometimes been very challenging for me, but it was very good for my development, and I am grateful for this experience.

I couldnt have done my experiments without the very thorough and kind help of Bettie Klomphaar, the biotechnician. She has supported me many times and her assistance in handling the animals and their precarious tissue is greatly appreciated. Furthermore, I am grateful to Gerco Hassink for providing me with tips in the lab and during recordings, and also for the discussions on a range of unrelated topics that came up during our lab days. Bettina Schwab was kind enough to advise me in the different stages of my project, and gave me new insights from a different perspective. I would also like to thank everyone else in the Biomedical Signals and Systems group for the opportunity to use their knowledge and experience.

During the time that I spent on my project, not everything could be serious, and I would like to thank all the students that I have had the pleasure of working with for their company and the many lunch and coffee breaks that helped me clear my mind. In particular I would like to thank Marc Schooneman for giving me extra feedback and providing a listening ear at the end of the day. As this project comes to an end, I realise once again how lucky I for all the opportunities I've had and all the wonderful people I have come to know. I would like to thank all my friends and roommates for the countless unforgettable experiences Ive had during my 7 years in Enschede, and naturally my parents for their patience and continuous support during my time as a student.

*–Freddy Gunneweg
May 18th 2015*

Summary

In order to measure neuronal activity in a controlled setting, microelectrode arrays (MEA) provide a multifunctional platform for various tissue preparations. Their capability to measure from many sites in the tissue simultaneously and with high temporal resolution makes them very suitable to measure activity from a network of interconnected neurons, for instance in cultured networks or in acute slices. Such analysis is especially relevant for research on Parkinson's disease (PD). It has been shown that due to the lack of dopamine in the basal ganglia, network activity in this brain area is severely affected, exhibiting excessive synchronization and oscillations. Although the exact mechanism behind this behaviour remains unclear, the striatum has been implied to play a major role in emergence of this pathological activity, because it is the input structure of the basal ganglia and the main target of dopamine. In investigations into how the striatum contributes to pathological oscillations, the MEA platform may provide a valuable tool for analysis of network activity.

The striatum mainly consists of medium spiny neurons (MSN), which are typically hyperpolarized but can be excited by coherent input from the cortex. The circuitry of the striatum is almost completely inhibitory, and is orchestrated by a small group of 'fast spiking interneurons' (FSI). These interconnected cells provide strong feedforward inhibition onto MSN's. Computational studies have shown in parkinsonian conditions, this network can nevertheless exhibit abnormal synchrony and oscillations as a result of compromised processing of cortical input. In *in-vivo* and *in-vitro* experiments, striatal MSN's are typically silent, but exhibit relatively depolarized states that enable action potential initiation. However, such experiments are either too complicated or too artificial. Acute slices may provide a more realistic yet stable simulation of the *in-situ* network and structure to investigate these patterns.

In the present study, slices of the healthy and parkinsonian striatum are investigated using MEA recordings. To this end, a test group of 7 rats was injected unilaterally with 6-OHDA, lesioning the substantia nigra to simulate dopamine denervation. Parkinsonian slices are expected to show higher firing rates and occurrence of bursts. However, in contrast with previous literature, no significant difference in firing patterns could be observed between control and lesioned animals.

During recordings, it was found that striatal tissue did not readily show spontaneous activity. Technical issues were assumed to be responsible, specifically the potential damage caused during slice preparation and the manual pressing of the slice onto the MEA chip. However, following protocol optimization, activity was still very sparse, presumably as a result of defects in the glutamatergic input from the cortex. Electrical stimulation and application of L-glutamine to the medium were generally not successful to provide sufficient excitation for long-term activity.

In order to provide a positive control for these measurements and to exclude technical issues, additional recordings were performed in the hippocampus, a brain region which is often used in acute slices and is typically much more active. Here, following recordings in the striatum, the hippocampus of the same slice was recorded, yielding much higher success rates. Spontaneous activity can be picked up immediately and could be measured for much longer durations. Additionally, in contrast with striatal recordings, activity was increased significantly following glutamine application, indicating that pharmacological stimuli are efficacious.

The results presented here show that in acute slices, cortical input is insufficient to excite striatal MSN's, although it was previously reported that individual corticostriatal connections were kept intact. This provides further proof for the hypothesis that striatal cells act as filters for cortical signals, firing only when sufficient correlated input is received.

Since the striatum is inherently inactive, it is difficult to determine during experiments if a slice is alive or dead, because external factors can easily cause cell damage and result in cell silence as well. A more powerful depolarizing stimulation should be applied to ensure that slices are viable. Following confirmation of slice survival, network activity should be recorded during simulating of cortical input, for example by electrical stimulation. However, this will likely entrain the network into an unrealistic state of activity, effectively masking the effects under investigation.

It can be concluded that although extracellular recordings on acute slices may be a promising method to simulate *in-vivo* tissue, this may not readily be applied to striatal tissue. However, recent findings in literature have suggested that following 24 hours of incubation, acute slices are able to restore their natural firing rhythms. Besides the practical benefits of recording a day after slice preparation, this would also solve the effective silence in future studies on striatal network activity.

Contents

1	Introduction	11
1.1	Recording network activity in acute slices	11
1.2	Motivation: origins of pathological oscillations in Parkinson's disease	11
1.3	Research questions	12
1.4	Project overview	12
2	Literature	13
2.1	Parkinson's disease: origins and treatments	13
2.2	Parkinson's disease and the basal ganglia	14
2.2.1	Modeling Parkinson's disease: Firing <i>rates or patterns</i>	14
2.2.2	Beta oscillations in the basal ganglia	14
2.3	The striatum	15
2.3.1	Oscillations in the striatum	16
2.3.2	Fast spiking interneurons in motor disorders and Parkinson's disease	17
2.4	Electrophysiological recordings in the striatum	18
2.4.1	<i>In-vivo</i> recordings	18
2.4.2	<i>In-vitro</i>	18
2.4.3	Microelectrode arrays	19
2.4.4	Acute slices on MEA's	19
2.5	Electrophysiological analysis	20
2.6	Hypotheses	21
3	Methods	23
3.1	Experimental	23
3.1.1	Chemicals	23
3.1.2	Animals and welfare	23
3.1.3	6-OHDA lesioning	23
3.1.4	Slicing	24
3.1.5	Hippocampus	24
3.1.6	Recording	24
3.1.7	Stimulation	25
3.2	Data analysis	26
3.2.1	Waveform analysis	26
3.2.2	Analysis of firing rates	26
4	Results	29
4.1	Clinical procedure and slicing	29
4.1.1	Protocol verification	29
4.1.2	6-OHDA model verification	30
4.2	Waveform analysis	30
4.2.1	Analysis of putative noise waveforms	30
4.2.2	Action potential characteristics	31
4.3	Recorded amplitudes and active channels	32
4.4	The striatum is not spontaneously active	32
4.5	Hippocampus provides positive control	33
4.6	Quantitative analysis of firing patterns	34
5	Discussion	35
5.1	Validation of setup: hippocampal slices	35
5.2	Technical factors in slice inactivity	36
5.2.1	Protocol	36
5.3	Physiological origins of cell silence	37
5.3.1	Recovering cortical input	37

5.4	Analysis of quantitative results	38
5.4.1	Characteristics of recorded signals	38
5.4.2	Obstacles in data analysis	39
5.5	Implications of results	40
5.5.1	Can FSI blocking be evaluated in acute slices?	40
5.6	Recommendations	41
5.6.1	Improving slice quality	41
5.6.2	Evaluating slice quality	41
5.6.3	Improving measurement setup	42
5.6.4	Improving data analysis	42
6	Conclusions	45
6.1	Slice inactivity	45
6.2	Acute slices	45
Appendices		
A	Electrophysiological recording of neuronal signals	55
B	Disregarded cluster templates	57
C	Local field potentials	59

Glossary

6-OHDA 6-Hydroxydopamine, used to lesion substantia nigra.

aCSF artificial cerebrospinal fluid, medium in which slices are incubated.

AP Action potential.

DA Dopamine.

DBS Deep brain stimulation.

EPSP Excitatory postsynaptic potential.

FSI Fast spiking interneuron.

FWHM Full width at half maximum (characteristic of waveform).

GPe/GPi Internal/external part of the globus pallidus.

IPSP Inhibitory postsynaptic potential.

ISI Interspike interval.

LFP Local field potential.

MEA Microelectrode array or multielectrode array.

MSN Medium spiny neuron, 95% of cells in striatum.

PCA Principal component analysis, used in spike sorting.

PD Parkinson's disease.

SNR Signal to noise ratio.

STA Spike triggered average, or template. Mean of spike waveforms in a cluster.

STN Subthalamic nucleus.

Chapter 1

Introduction

Parkinson's disease (PD) is one of the most prevalent neural disorders, second only to Alzheimer's. Estimates from the Parkinson's Disease Foundation indicate about seven to 10 million people worldwide are affected [1]. It manifests in movement defects such as slowness of movement and involuntary shaking (tremors), and can lead to mental illness like dementia and depression. The disease is degenerative and symptoms are usually diagnosed after the age of 50, incidence rates above the age of 80 can be as high as 5%. Public awareness for this disease has been greatly increased after public figures like actor Michael J. Fox and professional boxer Muhammed Ali revealed they had fallen victim to it. No cure has yet been found and current research is often aimed at finding ways to alleviate the symptoms. At the same time, it is imperative to gain more fundamental understanding of the complex mechanisms that underlie this neurodegenerative disease. In this project, the effects of PD are investigated at a cellular and network level, focusing on the role of fast spiking interneurons on abnormal neural activity in the striatum. This could lead to new forms of therapy for reversing the symptoms that arise in Parkinson's disease.

1.1 Recording network activity in acute slices

In order to understand neural activity in neurological diseases, it is possible to prepare neural tissue from lab animals, which can then be kept alive or even grown into a new network by incubating in a nutritious medium. At the BSS group, PD activity is investigated in **acute slices** of the rat brain. In this tissue preparation, the structure of the brain is largely maintained, which allows for analysis of fully developed brain tissue in a more stable setting. A commonly used technique to measure from acute slices is the patch clamp, which can selectively target individual neurons to measure their intracellular potentials and analyse their electrophysiological properties. However, this technique is very laborious and can only be used on few neurons simultaneously. Instead, **microelectrode arrays** (MEA) can be employed to record from many sites simultaneously in order to better understand how the network activity changes under different conditions. This makes this method a prime candidate to study PD *ex-vivo*. Here, MEA technology is applied to record network activity in the brain structure that is most associated with PD; the basal ganglia.

1.2 Motivation: origins of pathological oscillations in Parkinson's disease

One of the most striking features of brain activity associated with parkinsonism is that cells in the basal ganglia show excessive synchronized oscillations [2]. Neurons in the basal ganglia fire in phase and at specific frequencies from 10 to 20Hz. These 'beta' oscillations are likely a result of the complex feedback loops in this brain structure, yet the exact underlying mechanism remains debated. Nevertheless it has been shown that known PD treatments such as Levodopa and deep brain stimulation result in reduction of such abnormal patterns as well as significant amelioration of the cardinal PD symptoms. Additionally, beta oscillations have been linked to maintaining of posture in healthy animals, which provides a plausible connection to PD symptoms such as bradykinesia and rigidity. However, more research is required to understand how these network oscillations emerge and how they can be influenced.

Several structures within the basal ganglia might contribute to the excessive synchrony and oscillations. In this project, the main input structure of the basal ganglia is investigated: **the striatum**. Although this is not the main structure where DBS is most effective, it is the main target of SNc-released dopamine. It has been theorized that following dopamine depletion, the striatum alters its connectivity to other nuclei and becomes more active, which might trigger oscillations that are then amplified in the efferent nuclei.

A potential agent in the emergence of oscillations in the striatum is the **fast spiking interneuron** (FSI). Neurons of this type are known to form connections within the striatum and innervate large populations of neurons. FSI's are interconnected and may therefore play a large role in orchestrating pathological synchrony. However, experimental research into FSI's in the striatum has been limited to analysis of single neurons and connections. Several modelling studies have implicated that a network of FSI's in the striatal microcircuit may play an important role in striatal synchrony, but experimental evidence from network-wide investigations is missing. In order to fully understand the role of FSI's in PD, a controlled measurement setup is required in which selective targeting of cell types is possible in an accurate model of the striatum.

1.3 Research questions

Typical network experiments in the striatum are either performed *in-vivo* or *in-vitro* in cultured networks. While *in-vivo* measurements provide the most realistic measurement environment, the complexity of the brain often results in interfering processes. Conversely, cultured networks are grown from very young tissue, which has the ability to grow into entirely different network structures, possibly resulting in a change in input/output functions. To investigate network activity (e.g. beta oscillations) in PD, the striatal tissue needs to be fully developed and adjusted to the dopamine depletion. Acute slices therefore provide a more suitable model of PD conditions in a controlled setting. However, extracellular recordings in striatal slices have been sparsely reported, and it remains uncertain whether the slicing procedure significantly affects the recorded activity. If the acute slice is indeed an accurate model of the parkinsonian striatum, then extracellular measurements using MEA technology could provide a valuable new research method, and could provide new insights into how network activity can be influenced. This work is therefore also aimed at investigating the applicability of this electrophysiological measurement method. The main research questions are formulated as follows:

1. ***"Can we measure network activity in acute striatal slices on microelectrode arrays?"***
2. ***"Is there a measurable difference between the healthy and parkinsonian striatum?"***
3. ***"Is it possible to detect changes in the activity as a result of manipulating FSI activity?"***

1.4 Project overview

In order to appreciate the possible role of fast spiking interneurons in the pathology of Parkinson's disease, the cellular and network basis of the basal ganglia and striatum after dopamine depletion are studied in a literature review. The current understanding of how the basal ganglia react to dopamine loss is presented, focusing on the observations of excessive synchronized oscillations. An overview of the striatal microcircuit is given to suggest how oscillations can occur in this structure. Different lines of research implicating striatal roles are addressed, and evidence for a role of FSI's is presented, leading to the main research hypothesis on the function of FSI's in PD pathology. Finally, a set of experiments is described that aims to test this hypothesis by performing electrophysiological measurements in acute slices on microelectrode arrays. Verification methods are presented to compare results previously obtained in different brain areas.

Chapter 2

Literature

2.1 Parkinson's disease: origins and treatments

In 1817, Dr. James Parkinson was the first to publish an essay on the 'shaking palsy', in which he reports six cases of a degenerative condition characterised by resting tremor, abnormal posture and gait, paralysis and diminished strength [3]. Following Parkinson, Dr. Jean-Martin Charcot made further distinctions between the different symptoms that are collectively referred to as parkinsonism (fig. 2.1a); rigidity (stiffness), weakness and bradykinesia (slow execution of movement). Research soon found that this was a neurological disease, but the exact origin of the symptoms remained unknown. In 1938, it was finally asserted that the substantia nigra was the main affected brain structure, along with a large portion of the basal ganglia (fig. 2.1b). In 1960, Ehringer and Hornykiewicz published a paper describing the loss of dopamine (DA) in the striatum [4]. This was later attributed to the eventual death of dopamine-releasing neurons in the substantia nigra pars compacta (SNc), caused by abnormal accumulations of alpha-synuclein called Lewy bodies [5]. Selective lesioning of the SNc in animals [6, 7] results in realistic simulation of PD, leading to the notion that dopamine loss is essential in PD manifestation.

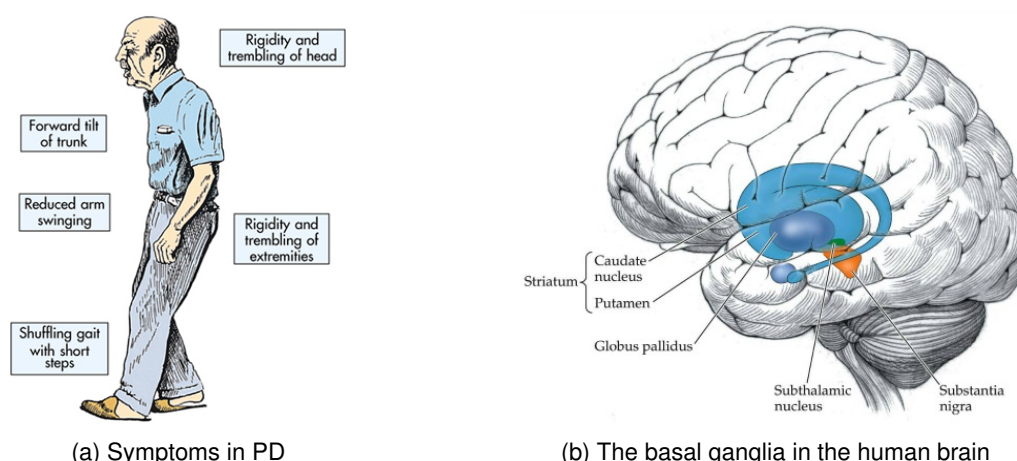


Figure 2.1: Symptoms and affected brain area in Parkinson's disease. *Left:* illustration of the most common effects of Parkinson's disease on movement and balance, including rigidity, slowness of movement and tremors. However, the disease does not have a footprint; patients can show many different variations of these symptoms. *Right:* PD mainly manifests itself in the basal ganglia. Signals from the cortex (top of the brain) move through the striatum to the globus pallidus and substantia nigra, which output to the thalamus. Dopamine release from the substantia nigra pars compacta is lost in Parkinson's disease, resulting in impaired signal processing in the basal ganglia.

In early stages after diagnosis, PD can usually be treated by increasing dopamine signalling, for example by intake of artificial DA replacement Levodopa or dopaminergic agonists such as apomorphine. However, side effects of DA increase result in different motor symptoms (dyskinesia) [8–10], and its efficacy decreases during PD progression.

In advanced cases where drug treatment fails, operative treatment by means of deep brain stimulation (DBS) can offer a solution. In DBS, parts of the basal ganglia are electrically stimulated, resulting in reduction of symptoms. Network activity is changed by DBS, but the efficacy of this method is empirical and has not been fully understood. Moreover, it is a very expensive and invasive procedure. In order to apply this therapy more effectively or to find alternative treatments, it is imperative that additional research is aimed at understanding how DBS affects the parkinsonian basal ganglia and why it is so effective at reversing PD symptoms.

2.2 Parkinson's disease and the basal ganglia

The basal ganglia (fig 2.1b) are a series of nuclei primarily associated with control of voluntary movement. They are located in the center of the brain and functions as a modulator of cortical signals to the thalamus [11]. The microcircuitry within the basal ganglia is very complex (see figure 2.2), but can be roughly distinguished in three communication loops. In the direct pathway, the striatum projects to the internal globus pallidus (GPI) and the substantia nigra pars reticulata (SNr), disinhibiting the thalamus. Conversely, striatal signals of the indirect pathway first pass through the external globus pallidus (GPe) and the subthalamic nucleus (STN) to increase thalamic inhibition by the GPI [12]. In a third 'hyperdirect' pathway, the striatum is altogether bypassed and cortical signals directly excite the STN. These two loops act antagonistically and can be considered a filter of cortical signals to the thalamus, thereby modulating movement.

2.2.1 Modeling Parkinson's disease: Firing rates or patterns

In the healthy basal ganglia, a balance exists between direct and indirect pathway activity, which results in regular motor behaviour. However, when parts of the basal ganglia are not functioning properly, for example as a result of targeted lesioning or in neurological movement disorders such as PD or Huntington's disease, this natural balance is disrupted, and it has been proposed that this is the underlying mechanism behind both dyskynetic and akynetic conditions [12–14]. In parkinsonian conditions, the gradual degeneration of the substantia nigra pars compacta has severe implications for the network activity of the basal ganglia.

In traditional models of the parkinsonian basal ganglia, it is theorized that the dopamine loss in the SNc leads to significant changes in the firing rates of the individual nuclei. As a result of such activity shifts, the thalamus effectively becomes inhibited. According to the rate model, the loss of dopamine modulation leads to disinhibition of striatal indirect pathway, which in turn causes increased inhibition of the GPe and disinhibition of the STN, which then promotes inhibition of the thalamus. Simultaneously, dopamine loss reduces inhibition on the GPI/SNr via the direct pathway, contributing to the inhibition of the thalamus.

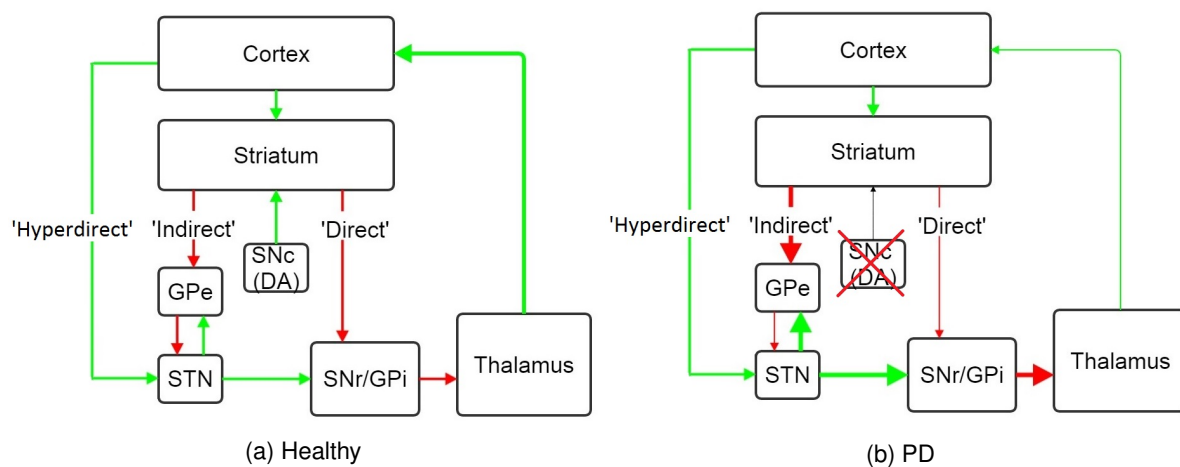


Figure 2.2: Model of the basal ganglia in healthy and parkinsonian state, as derived from [14]. Arrows indicate signalling pathways (green is excitatory, red is inhibitory, width is proportional to connectivity). Abbreviations: *GPe* - External part of the Globus Pallidus, *SNc* - Substantia Nigra pars compacta, *DA* - Dopamine, *STN* - Subthalamic Nucleus, *SNr* - Substantia Nigra pars reticulata, *GPI* - internal part of the Globus Pallidus.

While the firing rate model of PD in the basal ganglia has been widely used, it remains debated whether firing rates in specific nuclei actually change [15, 16]. The firing rate model predicts decreased GPI activity in hyperkinetic states, but firing rates were found to be close to those of the akinetic state [17]. Furthermore, lesions of the thalamus or the GPI do not result in the expected motor deficits [18, 19] but rather alleviated parkinsonism. Instead, changes in activity patterns are far more robust than expected changes according to the firing rate model, having been reliably detected in independent lines of research without exception. It has hence been proposed that firing *patterns*, not firing *rates* underly the parkinsonian state [2, 15, 20].

2.2.2 Beta oscillations in the basal ganglia

In classical control theory, unstable systems are often created by undamped feedback and feedforward loops, which can result in oscillatory behaviour. Since the basal ganglia form a similarly complex system, it could be expected that connectivity changes between the nuclei could result in similar instability [21]. Indeed, such oscillations are much more pronounced in recordings of parkinsonian rats, monkeys and humans [2]. Populations of neurons are found to burst more often at specific frequencies [22–24], most specifically in the beta band, around 10 Hz. Additionally, recordings of the local field po-

tential have shown increased oscillatory behaviour in the same regime [25, 26]. The band of observed frequencies ranges from 10 to 30 Hz, but exact frequencies differ between species. This could possibly be attributed to the difference in PD progression [2].

Causality with parkinsonism

Although neuronal oscillations are reported in all parts of the brain and have been deemed especially important in healthy functioning [27], the observed bursts in the parkinsonian state are especially abnormal and are considered to be a marker of PD pathology [28]. A causal link between oscillations and parkinsonism has yet to be proven, but almost undeniable evidence has been provided by the observation that all therapies currently available for PD treatment reduce oscillations [2, 29, 30]. Patients taken off their levodopa treatment show increased oscillatory behaviour [31, 32], while application of high frequency deep brain stimulation was found to suppress abnormal beta activity and simultaneously alleviate parkinsonian symptoms [33]. Conversely, stimulation with beta frequencies increased rigidity and bradykinesia [34, 35]. Taken together with findings that beta power increases in maintenance of position [36] and active movement suppression [37], and decreases during movement initiation, it can be concluded that beta oscillations support maintenance of motor states in the basal ganglia [38], and excessive beta is responsible for parkinsonian rigidity and bradykinesia. Interestingly, tremors are only marginally affected by beta activity [39], hence these symptoms may originate differently from rigidity and bradykinesia. It has been proposed that tremor is in fact created in the cerebellum, triggered by basal ganglia activity [40, 41].

Origins of synchrony and oscillations

Increased oscillatory behaviour is most prominent in the STN-GPe complex, which has consequently also been established as the most effective site for DBS therapy [42, 43]. However, excessive beta synchrony has also been reported in striatum [44–46] and GPi [24, 47] of parkinsonian animals. Therefore, it remains unclear whether this phenomenon arises from a single nucleus or from the activity of a specific nucleus in the basal ganglia. In recent modeling studies of STN and GPe, the pathological oscillations are demonstrated robustly [48–51], yet specific input changes of other nuclei are required for beta generation. Furthermore, lesioning of the GPe did not result in behavioural changes of MPTP-treated monkeys, nor did it evoke oscillatory bursting [52].

One remarkable notion that was ignored is that abnormal subthalamic activity is synchronized with cortical signals from outside the basal ganglia [53, 54], indicating that the basal ganglia do not act as an intrinsic pacemaker, but rather become more susceptible to external oscillations after dopamine depletion. A straightforward mechanism for this would be the hyperdirect pathway, which directly connects the cortex to the STN. However, models currently fail to identify how dopamine depletion results in excessive beta oscillations in the parkinsonian case. Furthermore, as Belluscio and colleagues [20] point out, the role of the striatum is excluded in this theory, while this structure is the main acting site of dopamine, and as such is heavily involved in the development of PD after dopamine depletion.

2.3 The striatum

As illustrated in figure 2.2, the striatum is the largest structure in the basal ganglia and serves as the first element in BG signalling. It is directly innervated by axons from the cortex and contains mostly medium spiny neurons which project to other nuclei. The striatum can be easily identified by the striato-pallidal projections, which can be seen as white bundles from the cortex inward. In most relevant literature, the term striatum refers to the dorsal part, consisting of the putamen and the caudate nucleus. Figure 2.3 shows the canonical model of the microcircuitry of the striatum, as presented by [55].

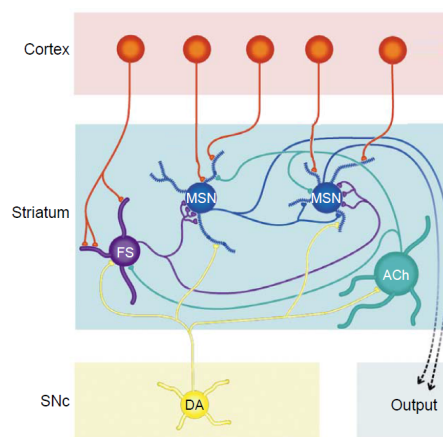


Figure 2.3: Canonical model of striatal microcircuitry, as given in [55]. The cortex innervates fast spiking (FS) interneurons and medium spiny neurons (MSN). MSN's receive input from FS and cholinergic (ACh) interneurons and project outward. Dopamine (DA) modulates cholinergic interneurons and MSN's. Synaptic connections are inhibitory, except for the glutamatergic signals from the cortex and dopamine signalling from the SNc, which is partly excitatory.

The vast majority of striatal neurons are medium spiny neurons (MSN) [56]; depending on the species the MSN population varies between 90% and 98% [12, 57, 58]. MSN's receive excitatory input via glutamatergic axons coming from the cortex and are inhibited by a variety of interneurons. Their output is GABAergic inhibitory and projects to other MSN's as well as the efferents of the striatum; the GPe and GPi. There are two subtypes of MSN's, and these incidentally make up the distinct signalling pathways of the striatum. MSN's expressing D1-type dopamine receptors make up the direct pathway, which can be excited by dopaminergic inputs. Conversely, D2-type receptors can be found in the indirect pathway; these are inhibited by dopamine. The two MSN types can be further distinguished by their expression of peptides such as enkephalin, dynorphin or substance P [59, 60]. Medium spiny neurons have a hyperpolarized resting potential, making them unlikely to fire [2, 61]. These cells have been found to fire irregularly and phasically, especially correlated with phases of depolarizing activity from the cortex and thalamus. MSN repolarization by inactivating potassium currents is rather slow, which results in typically wide action potentials with a significant overshooting effect, as observed in figure 2.4. This characteristic is often used to distinguish MSN's from other cell types [62–67].

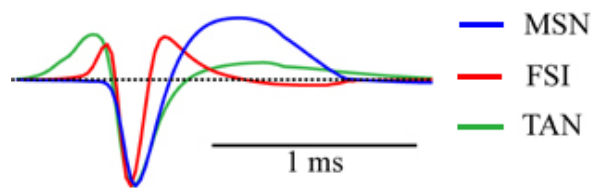


Figure 2.4: Characteristic waveform shapes of the different neuronal subtypes in the striatum¹. Tonically active neurons (TAN) are presumed to be cholinergic interneurons. Adapted from [67].

The remainder of striatal neurons have been identified to be a variety of interneurons, most notably cholinergic and GABAergic. Cholinergic interneurons innervate the population of MSN's and their activity is modulated by dopamine and other salient environmental stimuli [68, 69]. Cholinergic interneurons have a resting potential close to the spiking threshold, and as a result fire often [61]. This has resulted in identification of such neurons as tonically active neurons (TAN). It has been suggested that due to their specific ion channel properties, TAN's have the ability to generate activity autonomously [70, 71]. The effect of acetylcholine on striatal microcircuitry is relatively complex; interneurons innervate both MSN types as well as other types of interneurons [72]. They inhibit GABAergic interneurons via nicotinic receptors, while they inhibit MSN's via muscarinic receptors.

Although there are several types of GABAergic interneurons the most well-known type is the parvalbumin-expressing fast spiking interneuron (FSI), which makes up about 0.7% of the neostriatal interneurons in the rat [55, 57, 73]. FSI's are characterized by a tendency to strongly react to intracellular stimulation, although *in-vivo* activity is poorly characterized. Typical FSI firing patterns are irregular but can range up to 200Hz [55]. Additionally, FSI waveform shapes are typically short in duration [63, 74, 75], see figure 2.4. FS interneurons have been found to connect to each other via both electrical and chemical synapses [76], although they primarily innervate large populations of MSN's in the striatum in direct and indirect pathways [75, 77, 78]. Additionally, it has been shown that FSI's have little to no functional connections onto cholinergic interneurons or other GABAergic interneuron populations [75, 79–81].

2.3.1 Oscillations in the striatum

Since dopaminergic output of the substantia nigra mainly projects to the striatum, it is possible that this structure is responsible for the excessive oscillations in the basal ganglia. One theory is that the striatum acts as a filter that under normal conditions reduces harmonics generated in the cortex [20, 82, 83]. In the case of Parkinson's disease, this function is gradually lost, resulting in unwanted frequencies being passed to the rest of the basal ganglia. Synchrony and phase locking between cortex, striatum and STN have been observed across species [84, 85], and specific targeting of striatal NMDA gates was found to counteract the synchrony [82]. While the focus of this theory lies mostly on the slow-wave oscillations of ~ 1 Hz, it has also been proposed that other relevant frequencies might undergo the same filtering. Modeling work by Humphries et al has suggested that synchronized ensembles of MSN's occur following dopamine depletion and at beta frequencies.

An alternative theory for the role of the striatum is that it may act as an intrinsic pacemaker, generating the beta oscillations autonomously. The inhibitory nature of striatal circuitry would at first sight not hint at the possibility of pacemaking oscillations in the BG, since excitatory inputs would generally result in inhibition of efferent axons, effectively silencing the network. Nevertheless, oscillations have been reported *in-vivo* during task execution and cue utilization [62, 86]. The emergence of oscillations from

¹For information on the background of these signals occur and how they are measured, see appendix A

an inhibitory network may be attributed to the mechanism of post-inhibitory rebound spiking [87–89]. During an IPSP, the cell membrane tries to return to its natural balance, opening sodium channels to lift the potential. This will result in an overshoot of the membrane potential due to the time delay of the potassium gates. This results in a temporary depolarization which can lead to action potential onset. In this way, if multiple neurons are inhibited at the same time, they will rebound at the same time, leading to synchronization of silencing postsynaptic neurons, which will then follow the same cycle of rebound spiking.

To test whether postinhibitory rebound spiking was able to synchronize the striatal population of MSN's, McCarthy *et al* [90] modeled the activity of a network of MSN's, focusing on the M-current, a noninactivating potassium current with a relevant time delay to produce beta oscillations. They show that increases in inhibition of MSN's can lead to robust beta oscillations that become more pronounced if striatal ACh concentrations increase. Since dopamine modulates ACh release, this is a condition relevant to Parkinson's disease. The beta oscillations were less robust if the M-current was not included in the model. In order to verify their model, McCarthy *et al* performed an *in-vivo* experiment where they injected carbachol, a selective cholinergic agonist. This resulted in an increase in power in the beta frequencies of the local field potential (LFP). Injection of carbachol in neighbouring cortex did not evoke such oscillations. Effects of ACh on striatal output nuclei was not mentioned.

Although the results presented by McCarthy and colleagues strongly suggest a role for the striatum in eliciting beta oscillations, no unequivocal conclusions can yet be drawn about the exact responsible mechanism within the striatum. The increased acetylcholine in the striatum affects MSN's directly while at the same time silencing the fast spiking interneurons. This indirect effect has been dismissed, because in their model, networks of FSI's failed to produce abnormal synchrony under physiological parameters. Despite this, other research groups have reported evidence that would hint at a more substantial role for fast spiking interneurons in movement disorders such as Parkinson's disease. Most notably, work by Gittis *et al* has provided perspectives on the role of FSI's.

2.3.2 Fast spiking interneurons in motor disorders and Parkinson's disease

In a first line of experiments, Gittis and colleagues selectively inhibited fast spiking interneurons through selective targeting of specific receptors in mice, resulting in displays of dyskinesia (i.e. excessive erratic movement) [77]. Genetically modified mice were used to identify cell types in slices of the striatum and confirm selectivity of the drug IEM-1460 to block only FSI's and not MSN's or other interneurons. IEM targets calcium-permeable AMPA receptors which are only found on FSI's. As such, they block glutamatergic excitation and inhibit only FSI's. The results showed that this drug was able to dramatically reduce firing rates of putative FSI's, while MSN firing was unimpaired. Additionally, putative cholinergic interneurons showed only slight adaptations in firing rates, indicating that the drug could be used to test FSI effects *in-vivo*. After injection, subject animals started to display dyskinetic episodes which increase in severity with higher IEM-1460 concentrations. Additional experiments excluding cholinergic interneurons from participating in movement control did not produce such dyskinesia's, indicating that FSI's are the responsible neuronal species. Although the dyskinetic fits observed by Gittis are the opposite of symptoms associated with parkinsonism, it might be possible that FSI's have a significant modulatory effect on movement control by creating imbalance between the direct and indirect pathway.

In a second experiment, Gittis *et al.* shows that after injection of 6-OHDA, which triggers parkinsonian behaviour in mice and rats, FSI's rapidly increased their connectivity to indirect pathway MSN's while maintaining their connectivity to MSN's of the direct pathway. Again, neuronal cells were identified using GFP fluorescence of genetically modified mice; for each FSI that was patched, as many MSN's as possible were tested for connectivity before the FSI was lost. This resulted in a statistically relevant difference in connectivity that was rapid and persistent over as long as 4 weeks. The authors also present a simple integrate-and-fire model of FSI's and both D1 and D2 MSN's, and show that the observed increased connectivity between interneurons and indirect MSN's can lead to synchronization of the indirect pathway. However, oscillatory mechanisms have not been reported, and the beta regime was not discussed. Furthermore, no experimental evidence was given for an increased synchronization of D2 MSN's.

FSI's have been further implicated in Parkinson's disease by findings that their excitability is reduced after dopamine depletion [91]. This could potentially form a mechanism by which dopamine depletion reduces striatal filtering of cortical oscillations, since the MSN excitability is consequently increased. Additionally, several modeling studies have suggested that FSI is essential to normal striatal activity, and that reduction of FSI input leads to overactivation of D2 MSN's [92] and might also lead to generation of beta synchrony [93]. Interestingly, FSI's are also considered capable of synchronising large populations of MSN's under normal conditions, given their large axonal innervation and their capability to communicate in an FSI-network via electrical gap junctions.

2.4 Electrophysiological recordings in the striatum

In order to investigate the effects of dopamine depletion in the parkinsonian striatum, different levels of analysis can be used for experiments. Cellular analysis is employed to investigate the specific reaction of cell types to pharmacological manipulation, or to describe fundamental principles of neuronal processing such as synaptic plasticity. Conversely, network analysis requires measurements from multiple neurons simultaneously, to investigate how ensembles of neurons process input stimuli. This type of analysis is especially relevant to understand network oscillations and synchrony in the striatum. Finally, behavioural analysis can be used to understand how neuronal activity affects behaviour of the subject, for example motor deficits in PD.

Experiments in the striatum can be done *in-vivo*, *ex-vivo* in acute slices and *in-vitro* in cultured networks. Each of these physiological models has advantages for different forms of analysis. Current literature reveals that research in the striatum has mainly focused on characterizing individual cells and connections, as well as functional effectiveness of applied drugs. However, experiments on network effects in the striatum have been few in number, and mostly performed *in-vivo*. In this section, several techniques for electrophysiological measurements are discussed, and the choice for employing microelectrode arrays and acute slices is motivated.

2.4.1 *In-vivo* recordings

The development of implantable microelectrodes has enabled *in-vivo* recordings of neuronal activity with single neuron resolution [94] from areas further into the brain, such as the striatum. This allows for direct correlation of neuronal activity and function to gain insight in motor control, sensory perception and sensorimotor learning. Similarly, stimulation of brain areas can be used to alter memory [95], suppress motor deficits [96] and epileptic seizures [97], or to provide feedback in a brain-machine interface [98].

In-vivo measurements provide the most realistic environment for signalling in the brain, which allows for analysis of functional effects. Additionally, extracellular potentials of neuronal ensembles and local field potentials can be used to study network effects on specific brain areas. However, *in-vivo* experiments are not set in a stable environment, and complex background activity (e.g. heartbeat, breathing, and global network dynamics of the brain) interfere with the desired responses. Furthermore, such procedures are relatively difficult to maintain due to inaccurate placement of the electrodes and electrode drift during movement.

2.4.2 *In-vitro*

In order to more clearly understand the interactions in the striatum in a more stable setting, neuronal networks of striatal tissue can be cultured *in-vitro*. In such procedures, striatal tissue is extracted from postnatal rats and placed in medium which promotes cell growth and activity. This leads to formation of new neuronal structures over the course of 30 days, and creates an 'artificial' striatal network with similar characteristics as observed *in-vivo* [99]. These organotypic cultures have been used to successfully study activity of both medium spiny neurons and fast spiking interneurons.

Although many of the activity characteristics of the striatum in organotypic slice cultures strongly resemble activity seen *in-vivo*, it remains uncertain whether the network behaves in a similar way. Because the slices in these networks are still underdeveloped at the time of extraction, they will form alternative structures as a result of their placement *in-vitro*. In order to investigate the striatum in its mature form *in-vitro*, acute slices can be prepared from mature rats. In acute slices, the brain is already fully developed, and connections in the basal ganglia can be kept intact [100]. Furthermore, this model can be used to study effects of specific lesions outside the striatum, for example to the substantia nigra. In organotypic cultures, the effect of such lesions will not impede neuronal growth, and hence may result in different networks. It is for these reasons that this project focuses on studying the parkinsonian striatum in acute slices.

Intracellular recordings

Several techniques exist to measure extracellularly and intracellularly from the striatum *in-vitro*. Intracellular experiments can be applied using a patch-clamp setup. This setup can be used to record spontaneous and stimulated activity from individual cells, which have to be selectively patched using a pipette electrode. Mechanical suction or electrical stimulation can be applied to attach to the cell membrane and measure/manipulate the medium locally. Typical setups can patch one or two cells simultaneously, providing high signal to noise and target-selectivity to investigate individual cell properties or single connections between cells. This has led to improved understanding of FSI and MSN characteristics and was used to prove effectiveness of drug application (e.g. IEM-1460 selectivity in [77]).

While intracellular experiments allow for stable investigation of single neurons with high signal to noise ratios, it is generally not possible to measure from more than two neurons simultaneously. In order to investigate network activity, recordings from multiple sites in the network are required to measure correlations and potential oscillations and synchrony. This can be done using planar microelectrode arrays.

2.4.3 Microelectrode arrays

In recent years, planar microelectrode arrays (MEA) have become the standard for more stable *ex-vivo* and *in-vitro* recordings of neuronal networks [101–103]. Miniaturization in semiconductor technology has led to production of microelectrodes that are capable of measuring electrophysiological signals with high signal-to-noise ratios and at great spatiotemporal resolutions. Such chips can be used to record from acute slices of the brain or from cultures of dissociated neurons. Commercial MEA's are available that contain ~ 60 electrodes and can simultaneously measure and stimulate neurons (e.g. Med64, Multi Channel systems). Further research has presented opportunities to create high density MEA's (HDMEA), which have over 10.000 electrodes capable of measuring at subcellular resolutions [104, 105].

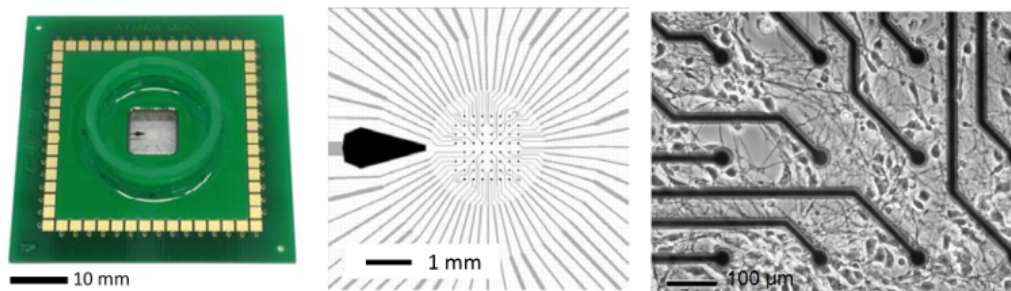


Figure 2.5: Example of a microelectrode array chip, as used in this experiment. The platinum electrodes are deposited on a glass substrate, which is glued to a circuit board, providing connections to an amplifier. A glass or PDMS well is glued to the board to provide a recording chamber. *Middle*: Layout of the electrodes on the glass chip, with a large reference electrode located on the left-hand side. *Right*: Microscopic image of neurons on the chip (dark spots close to electrodes), as observed in a cell culture. Electrodes can record from single neurons, but also from aggregates (left top), where mixed signals from multiple neurons are simultaneously recorded. From Qwane Biosciences, Lausanne.

Because the electrodes are spread over an area of about 1mm^2 , it is possible to record from multiple locations in a network. Provided that the connections in a slice remain intact, this enables more widespread recordings of neural networks. In this project, MEA technology allows for simultaneous recording of multiple neurons in the striatum, leading to better understanding of how the striatal population reacts to stimuli.

Such stimuli, both chemical and electrical, can easily be applied using this technology. MEA's are typically packaged on a PCB chip with a PDMS or glass well on top, as seen in figure 2.5, in which the neural network is placed in a bath of nutritious fluids that support neural activity. This setup allows for precise control of chemical composition in the bath, which can be used to study drug efficacy and the role of neurotransmitters in the brain. Such studies are especially relevant for the investigation on PD, since this has previously been treated both chemically and electrically, thus new treatments can more easily be compared in a stable setting. *In-vivo*, pharmacological treatments are harder to administer because of the blood-brain barrier, which is absent in acute slices.

2.4.4 Acute slices on MEA's

Acute slices have been used extensively to study synaptic plasticity in the hippocampus, both intracellular and extracellular, and serve as a main model for cortical pyramidal cells. The hippocampus is a brain area with a very well-defined layered organization (figure 2.6). The morphology and orientation of pyramidal cells in the CA1 and CA3 area's are easy to identify, and connections between these area's (Schaffer collaterals) have been shown to be fully functional in transverse hippocampal slices, with minimal damage to the dendritic arbor and axon collaterals [106]. Schaffer collaterals have been successfully targeted using MEA's [107, 108] and procedures for obtaining hippocampal slices have crystallized into generally accepted protocols.

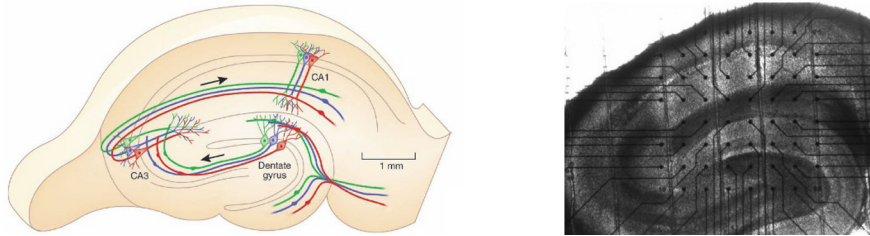


Figure 2.6: Functional connectivity in the hippocampus. *Left*) Schematic of signalling pathways in the CA3, CA1 and dentate gyrus shows that neurons are neatly aligned and can therefore be easily identified (from: [109]). *Right*) Image of an acute hippocampal slice on a MEA surface, which shows that MEA technology can be used to stimulate CA3 and measure in CA1 to study plasticity of Schaffer collaterals (from: Multichannel Systems).

In comparison, extracellular measurements on acute slices of the striatum are very rarely reported [110, 111], and no quantitative information regarding spontaneous activity in striatal slices was reported. Intracellular measurements in the striatum have been widely employed to study individual connections [55, 77], and it was reported that connectivity between nuclei in sagittal slices of the basal ganglia could be maintained [100]. However, little is known regarding the network activity in acute striatal slices, since intracellular experiments are performed in individual neurons and only viable neurons are reported. Furthermore, since nuclei in the basal ganglia are intricately interconnected, cell activity in the striatum may be much more dependent on external inputs from other nuclei, especially compared with the hippocampus which can be recorded in complete isolation from the rest of the brain. It is therefore unsure how much activity can be expected from MEA recordings in striatal slices.

2.5 Electrophysiological analysis

Microelectrode array recordings are capable of measuring from several neurons simultaneously, because extracellular potential fields of neighbouring neurons overlap and can be summed. In order to evaluate spike time dependencies between neurons (for example in case of synchrony), it is necessary to properly assign recorded action potentials to their sources. This process of spike sorting is based on the assumption that due to unique membrane properties and contacts with electrodes, each neuron has a distinguishable waveform shape. In order to capture this difference, many attempts at providing a set of distinguishable features have been attempted, for instance the full width at half maximum (FWHM), peak-to-valley or rising phase of the repolarizing current [77, 112–114]. Alternatively, automatic feature extraction using principal component analysis could be used to find optimal distinction features based on the characteristics of the recorded waveforms themselves [115]. Evaluating the features of each waveform, algorithms should identify clusters in the feature space, these clusters are regarded as individual sources (i.e. putative neurons). Depending on the nature of the feature distribution, different clustering schemes may be applied (examples include Gaussian mixtures/expectation maximization, k-means, superparamagnetic and mean-shift clustering).

Although automatic algorithms for spike sorting and classification exist, they are often far from ideal and therefore typically require manual supervision [115]. However, in the case of MEA recordings where each channel has to be separately analysed, this is too labor intensive. Since the circumstances of each channel (noise levels, active time lengths, cell contacts) are different, algorithms should be self-learning and data analysis should be flexible to accommodate different modalities of data, preferably with as few parameters as possible to prevent system bias. Statistics of the results can then be used to determine the quality of the sorting, for example by counting violations of physical boundaries, or by evaluating distribution of waveform amplitudes [116].

In order to analyse network activity from multiple electrodes in the tissue, several techniques may be employed. Firing rates can be readily analysed by evaluating the inter-spike interval (ISI) of the spike-sorted neurons. However, in most cases these firing rates are not constant. Neuronal signals often fire in irregular patterns, showing single spike activity or bursts of action potentials. As a result, analysis of the firing rates depends on the patterns in the signal. In [117], a method to distinguish between different firing patterns is presented, in which a histogram is made of the number of spikes in a given time bin. The length of these time bins is equal to the mean ISI, in order to accommodate both high and low frequency signals.

In order to understand how firing patterns are oscillatory, inter- and intraburst intervals should be evaluated. In [20], it is theorized that following dopamine depletion, striatal neurons become more excitable during striatal UP-states, which would result in occurrence of bursts intermitted by silence, whereas activity in the healthy striatum should only exhibit single spikes (figure 2.7). Similar results were obtained from striatal slices in [110]. Because bursts can be scattered very heterogeneously, detection of these bursts can be complex. Several strategies for burst detection have been presented, which can easily be applied to the MEA recordings [117–119].

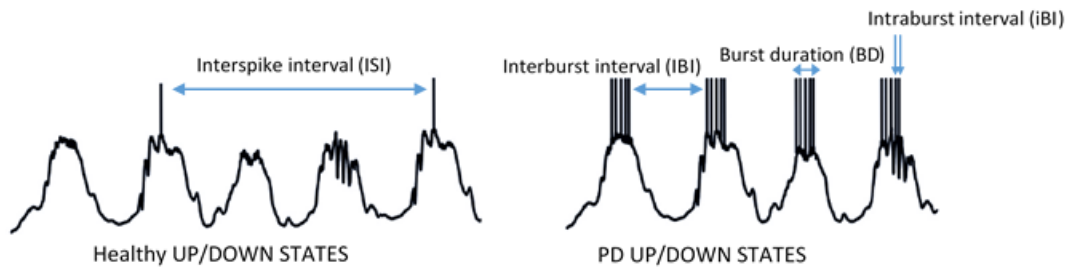


Figure 2.7: Measures for characterizing signal activity in the striatum. In healthy striatum, signals are expected to be irregular without bursts, while signals in the parkinsonian striatum are expected to show bursts, of which the interburst interval and intraburst interval can be calculated. Figure adapted from [20]

For further evaluation of synchrony in the neuronal networks, crosscorrelograms can indicate whether spikes from two different neurons are correlated. However, these pairwise correlations are not necessarily representative of network synchronicity [120]. Neuronal synchronization and oscillations can more readily be observed in recorded local field potentials [2]. LFP's are summations of extracellular potentials, including subthreshold fluctuations. Fluctuations of single cells are too indistinct to significantly alter the LFP. However, when groups of neurons are depolarized simultaneously, this can cause substantial peaks in the LFP. Spectral analysis (such as spectrograms, power spectral density) can be employed to quantify synchrony and oscillations in neural networks.

2.6 Hypotheses

In the previous section, several important lines of evidence were presented:

1. The striatum has a major role in synchronizing the basal ganglia, either by filtering of cortical signals [20] or by intrinsically generating beta oscillations after dopamine loss (McCarthy: [90])
2. Fast spiking interneurons affect movement disorders and change connectivity in PD (Gittis: [77, 121]).

This project will be aimed at the role of the FSI's on network activity. Although McCarthy *et al* implied that fast spiking interneurons are silenced by increased acetylcholine expression, the possibility of FSI influence on oscillatory behaviour has not been explored. Nevertheless, this effect may contribute greatly to the network synchronisation, especially due to the high FSI-to-MSN connectivity. On the other hand, reduction of FSI inhibition might increase activity in the striatum, leading to reduced filtering of cortical input.

Following Gittis *et al*, FSI's could be blocked by applying IEM-1460. In acute slices, this method was used intracellularly, but spontaneous effects on spontaneous activity in the network were not discussed. Since the striatum is expectedly less active in acute slices than *in-vivo*, it is unsure if and how well activity in these slices can be manipulated. However, previous results using MEA recordings have shown that the 6-OHDA rat slice exhibited more bursts and fired more frequently [110]. Hence the following hypotheses are formulated for experiments in the striatum:

- In the healthy striatum, activity is low, but FSI blockade is expected to increase excitability and neuronal activity.
- In the parkinsonian striatum, baseline activity is increased, and more bursts are expected.
- Beta oscillations are expected to be observed in the striatum of parkinsonian animals.
- Synchronized beta oscillations are increased after inhibition of FSI's in the parkinsonian striatum.

Chapter 3

Methods

3.1 Experimental

In order to understand the effect of manipulating fast spiking interneurons on the network activity of the striatum, a controlled environment is required. The microelectrode array technology is especially well-suited for this project, because it allows recording from multiple sites and can also facilitate electrical stimulation, as well as controlled drug delivery.

As a model for Parkinson's disease, the brain of a rat is lesioned with 6-OHDA, effectively destroying dopamine-releasing neurons in the substantia nigra. This requires mature animals, which should have developed a stable brain function in the absence of striatal dopamine. The experiments will therefore be performed in acute slices of the striatum, which provide the best ex-vivo approximation of the in-situ striatal microcircuitry.

Because this work is one of few investigations using acute slices of the striatum on a MEA, additional recordings will be performed in the hippocampus. This is a relatively well-known brain structure with clear morphology and intrinsic activity, and similar experiments have been previously performed in such preparations. These experiments will serve as a control setting to validate the protocols. Protocols for slice preparation and maintenance have been adapted from the Multichannel Systems application notes on the hippocampal slices.

3.1.1 Chemicals

Chemicals were obtained from Sigma Aldrich (Zwijndrecht, NL) unless otherwise stated. Rat brains are kept and sliced in artificial cerebrospinal fluid (aCSF). During brain extraction and slicing, a cutting medium is used that reduces activity excitotoxicity during cutting, while slices are allowed to recover in recording medium. Cutting medium contains 75 mM sucrose, 87mM NaCl, 0.5mM CaCl₂, 7mM MgCl₂, 2.5mM KCl, 1.25mM NaH₂PO₄, 25mM NaHCO₃, 25mM D-glucose and 1mM ascorbic acid. Recording medium contains a higher concentration of NaCl (125mM) and a higher ratio of CaCl₂ to MgCl₂ (respectively 2mM and 1mM). aCSF made fresh on the day of experiment and during experiments is continuously bubbled with carbogen (95% O₂, 5% CO₂) to provide neurons with oxygen, as well as maintain a pH of 7.4.

3.1.2 Animals and welfare

All animals are treated with the highest care and handled according to the guidelines of the Dierexperimentencommissie (DEC) and Dutch law. Wistar rats of at least 3 weeks old are used for experiments in control groups, while the PD animals are 2 months old or at least 350gr. To avoid influence of oestrous cycle, only male rats are used.

3.1.3 6-OHDA lesioning

As a model for PD, a group of 9 rats is unilaterally injected with 6-OHDA in the substantia nigra of the right hemisphere. Rats are anesthetized under isoflurane and injected with desipramine and pargyline to block 6-OHDA from affecting the body and to prevent unwanted metabolism of 6-OHDA. They are then mounted in a stereotaxic setup under isoflurane anesthesia. Injections of 4μL 6-OHDA (2μg/μL) in saline solution are administered via a cannula in the medial forebrain bundle. Following injection procedure, lactated Ringer's solution is given to ease recovery. Experiments are performed in four to six weeks after the operation.

Several behavioural tests are used to confirm parkinsonian state. One week before injection and one week before the recording experiment, animals are placed in a transparent cylindrical container, and the number of rearings is counted. Additionally, an open field test is performed for 10 minutes in a box of 1 square meter with 9 grids. In post-operative tests, apomorphine (0.25mg/mL/kg) is injected subcutaneously, which should result in excessive contralateral turning as a result of dopamine agonistic action. Since all of the tissue is used during recordings, no immunohistochemistry is performed to verify the extent of the lesion.

3.1.4 Slicing

One hour before preparation, animals are given an injection of carprofen as a preventive pain alleviation. They are then anesthetized under 5% isoflurane, followed by intracardial perfusion with ice-cold oxygenated cutting solution for 3 minutes. The rat is then decapitated and the brain is extracted. The brain is washed in aCSF and allowed to cool down for about 1 minute. The cerebellum is removed using a razor blade and the lateral edges are removed. The brain is then cut mid-sagittally, glued to a holder for slicing (lateral side is upward) and kept in ice-cold oxygenated aCSF. Sagittal slices of 300 μ m thickness are made using a vibratome (Leica VT1000s) at 80Hz vibrating speed and a translational velocity of 0.125mm/s. The knife is put at an angle of 15°, so connections from cortex and to STN, GPe and GPi are maintained, as previously verified. Fresh slices are placed in recording solution and warmed up in a waterbath, which is set to 36°C after transferral. This allows cells to slowly equilibrate and restores activity in the slices.

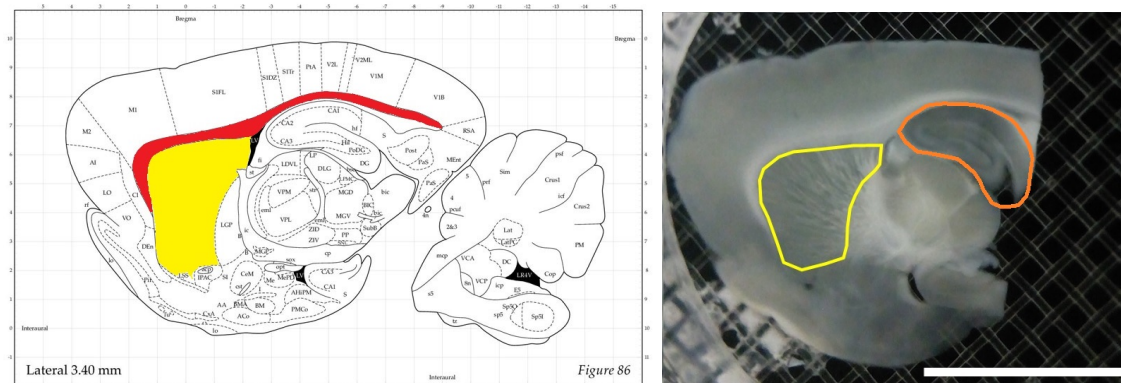


Figure 3.1: The striatum in sagittal slices of the rat brain (scalebar: 1 centimeter). *Left:* The rat atlas clearly shows the striatum (yellow) positioned just under the corpus callosum (red). *Right:* These structures can easily be identified in slices that were obtained during experiments, where the striatum (in yellow) is further characterized by the white lines of axons that give it the striated look. Note that in the slices, irrelevant brain parts on the right (including the cerebellum) were cut off to maintain slice integrity. However, the hippocampus can still be identified in orange, with its clear layered structure.

3.1.5 Hippocampus

In order to provide a positive control slice activity, parasagittal slices are moved after recording in the striatum. The hippocampus is placed on the MEA surface, and the mesh is placed back. Although structural quality is lower in the hippocampus as a result of the slicing procedure, it can still easily be identified according to its layered structure of CA regions (see orange labeled region in figure 3.1). In order to obtain better quality of the hippocampus, slices from one healthy animal were prepared in the transverse plane, since lamellae of the hippocampus are thought to lay in this orientation [122]. This was done by making a horizontal plane with a knife and using that plane as the base of slicing. Slices are cut from lateral to medial side at the same angle of 15°, as adapted from the MC application note.

3.1.6 Recording

Neuronal recordings are recorded on a 3D microelectrode arrays (Qwane, Lausanne), which consists of a 8x8 matrix of pyramidal platinum electrodes on a glass substrate (four corner electrodes are not active). The shape of these electrodes allows them to pierce through the layer of dead neurons and make a better connection to active neurons [107, 123]. The electrodes, spaced at 200 μ m, are conical with a diameter of 30 μ m and height of 50-70 μ m, resulting in an impedance of 450-650k Ω . An internal reference electrode is located on the left side of the chip.

Before recording, MEA's are cleaned in biotex and kept in Milli-Q water to make them hydrophilic. During experiments, slices are carefully laid on top of the electrodes and then perfused with aCSF. Slices are compared with the rat brain atlas (Paxinos & Watson, 6th edition, Elsevier) to identify and selectively record from the striatum (see figure 3.1). To provide better contact with the electrodes, a ring with a fine mesh grid is laid on top and can be pressed down with a micromanipulator (Green Leaf Scientific, Ireland), which consists of a spring that can be pressed down using a fine screw. The recording chamber is continuously perfused with aerated aCSF at a rate of \sim 1.5-2 mL/min. MEA's are placed in MEA2100 headstage (Multichannel Systems GmbH, Reutlingen, Germany). A custom 3D-printed cap fitting is placed on top of the headstage to hold perfusion needles and the micromanipulator in place (see fig. 3.2). Fluid inflow is first heated using a perfusion cannula, and the recording chamber is kept at temperature using the heating element in the headstage. Heat conduction is increased by using a metal spacer between the heating element of the headstage and the MEA chip.

To eliminate electrical noise, the perfusion needles and cannula are grounded to the head stage. Grounding of the micromanipulator increased noise as a result of vibrations in the spring. Instead, the micromanipulator is isolated using a rubber seal to prevent it from behaving as an antenna. In the headstage, MEA signals are amplified, bandpass filtered (1Hz-3.3kHz) and digitized at 25kHz. Signals are then visualized using MCRack, and a threshold of minus 5 times the RMS noise value was set for each channel. The threshold cannot be updated during a recording. If the data signal crosses this threshold with a negative slope, a data waveform of 4ms, centered around a threshold crossing, is recorded. These waveforms will also be referred to as 'spikes'.

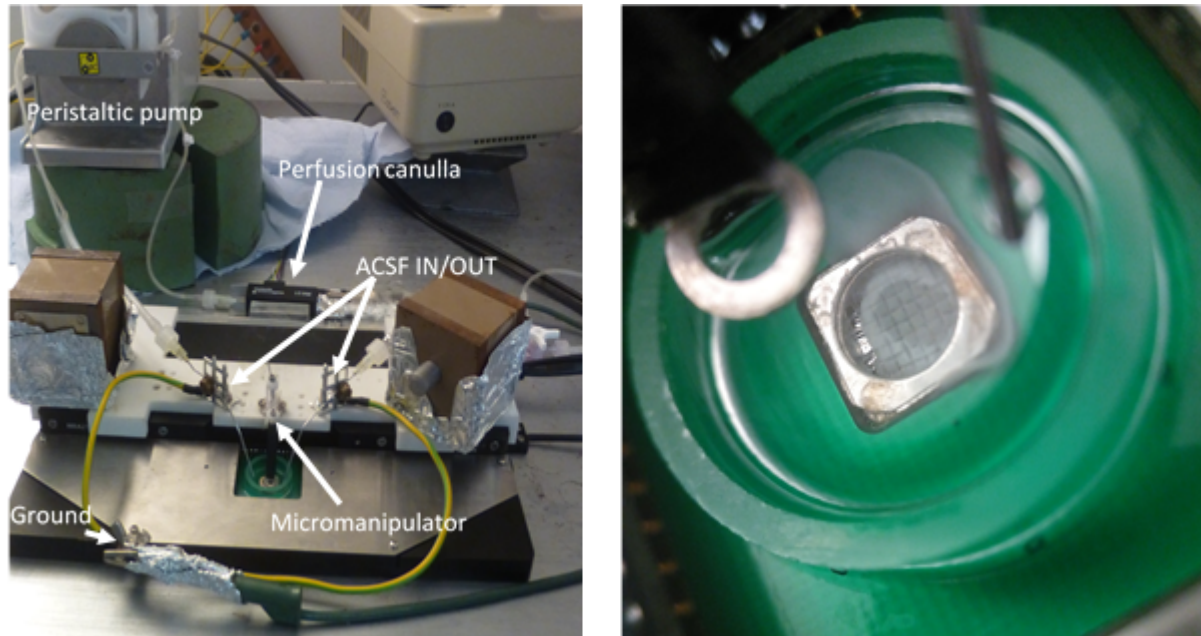


Figure 3.2: Setup for recording from acute slices. *Left*) A custom fitting is placed on top of the mainstage to provide a platform for the perfusion needles and micromanipulator. Metal weights are placed on top to provide better contact and to prevent movement. *Right*) A custom mesh is placed on top of the slice, which is held in place using the micromanipulator. This provides more uniform pressure on the slice.

3.1.7 Stimulation

In order to stimulate the tissue, mechanical pressure was applied lightly so that slice contact is sufficient. Electrical stimulation was applied on one electrode just out of the center of the MEA. Biphasic pulses of -1V/+2V for 1ms were applied every 10 seconds at a center electrode for two minutes to evoke action potentials. This results in a stimulation that is observed on all electrodes, but is slightly attenuated at electrodes on the edge. This also serves to verify that slice contact is sufficient, because stimulations propagate further when there is a slight gap with ACSF between MEA surface and slice.

Alternatively, high frequency bursts of pulses (130Hz) were applied. The propagation of the electrical stimulation across the chip was used to confirm contact, because the contact with the slice will decrease the electrode-tissue impedance.

When no clear threshold crossings could be observed in the signal, slices were further stimulated by applying more pressure on the mesh. This should result in activity to verify that slice contact is sufficient. To further enhance activity in the striatum, L-glutamine is occasionally added to the solution, in dosages of 1mM to 15mM. Fluid flow is redirected from a separate tube containing the modified aCSF. Alternatively, L-glutamine (3-5mg) is sometimes directly applied to the recording chamber to elicit a stronger reaction. Additionally, IEM-1460 (Tocris Bioscience, 50 μ M) is occasionally added to the medium to inhibit FSI's [77].

3.2 Data analysis

Data analysis is performed using Matlab r2014a (Mathworks). Data consists of recorded waveforms and in some cases, raw electrode data. Waveforms are analysed to find firing patterns, while raw electrode data is used to analyse local field potentials and to verify the selection of waveforms.

3.2.1 Waveform analysis

Figure 3.3 shows the overview of how waveforms are analysed and how signals are separated. In order to separate action potentials from noise waveforms, irrelevant spikes are rejected. First, a coarse artefact rejection is performed based on waveform amplitude and timing. Spikes occurring simultaneously (within are assumed to arise from external sources (e.g. air bubbles of aCSF perfusion, background vibrations). Stimulation artefacts are characterized and rejected based on the 'flat' signal preceding the spike as a result of the blanking circuit. Additionally, waveforms that exceed a threshold of $50\mu\text{V}$ at the beginning and end of the waveform shape are disregarded, as spikes are expected to fall to baseline level within 1 ms. Finally, if the signal amplitude of a waveform is higher than $80\mu\text{V}$, it is discarded as noise.

Following artefact rejection, a spike sorting algorithm is applied to filter signals from multiple sources. This sorting is based on the assumption that waveform shapes of a single neuron are distinct and constant, as a result of the unique membrane properties and the contact with an electrode. To find the defining features of distinct waveform shapes, singular value decomposition (SVD) is applied to project each waveform to a multidimensional feature space. Using principal component analysis (PCA), the features that have the highest variance are selected to perform waveform clustering. These principal components are thought to best capture the minimal set of features required for distinction of the different groups of waveforms. In the final script, 5 principal components are selected for spike clustering, as this was experienced to deliver accurate results.

A meanshift clustering scheme [124] is used to estimate a probability density function (PDF) to the PCA space and find the local maxima in this function. This is done by shifting the PDF estimate within a bandwidth and assigning spikes to the nearest maximum. Because signals from each electrode are analysed independently, a high degree of autonomy is preferred to reduce the need for manual intervention. The meanshift algorithm requires only one parameter to be set: the bandwidth. It will automatically determine how many clusters should be found and is independent of the shape of the density function. However, depending on the number and distribution of data points in the PCA space, this bandwidth should be set higher or lower. Here an iterative bandwidth selection is performed. If, following the first clustering cycle, only one cluster is found with a high number of waveforms, the bandwidth is reduced to prevent overclustering. Similarly, complete underclustering (each waveform is a cluster) is prevented by iteratively increasing the bandwidth. The settings of the iteration are such that underclustering is preferred to overclustering. In this way, signals should not be clustered together with noise, but multiple signal clusters may result from one signal. Clusters with less than 3 waveforms are considered outliers and hence discarded.

Finally, the algorithm aims at automatically classifying whether the clusters that were found consist of physiological signals. Noise waveforms resulting from errors in the threshold are often measured, which will influence the statistics of spiketime analysis. In order to reject such results, the spike triggered average (STA) or template is evaluated. Noise waveform shapes often display discontinuities, lack overshoot and generally have small wavelength. Clusters with such templates are rejected by applying a series of conditions on the waveform shape. Waveforms are labelled according to the length between peak and valley, as well as their full width at half maximum (FWHM) and signal to noise ratio (SNR). Clusters where the STA does not cross the zero line are discarded, and a threshold to the FWHM is set. Additionally, clusters where peaks (local maxima with more than 0.5 times the maximum amplitude) are detected in the beginning or end of the waveform are also rejected. When the minimum of the template is more than 0.8ms from the center of the window, or when the amplitude of the template is less than $15\mu\text{V}$ and the overshoot is less than 20% of the maximum amplitude, then the signal is considered monophasic and rejected.

3.2.2 Analysis of firing rates

Firing patterns are categorized using the discharge density histogram [117], to which a Poisson-distribution and a Gaussian are fitted. If the fit of the Poisson distribution is significant, then the pattern is classified as 'random'. A significant Gaussian fit classifies the signal to be 'regular', otherwise the signal is considered 'bursty'. To ensure sufficient resolution for the histogram, only signals with more than 15 spikes are classified. Maximum firing rates are approximated by calculating the first quartile of the interspike interval (ISI) of each neuron and taking the inverse. Spike counts per minute, inter-burst, intra-burst intervals and burst durations are also collected and compared between lesioned and healthy slices. Burst characteristics are determined using methods introduced in [118]. Bursts are detected using the

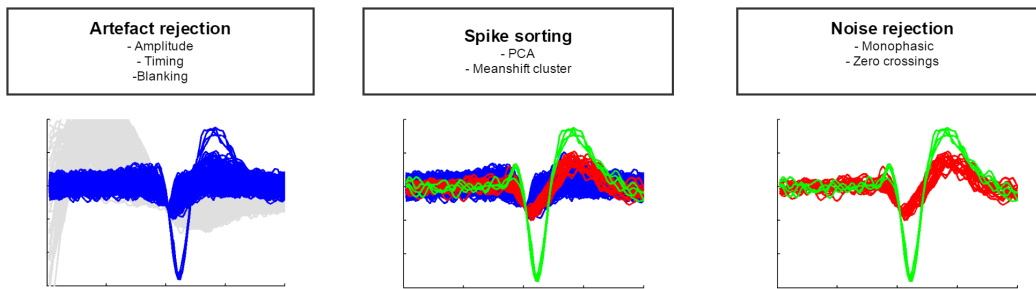


Figure 3.3: Steps of the waveform analysis. 1) Overview of detected waveforms shows that there are distinct groups, but a significant portion of spikes is due to electrical stimulation. These spikes are rejected based on spike timing. 2) Remaining spikes are clustered according to their waveform shape using a PCA scheme. 3) Nonphysiological waveform clusters are rejected based on their waveform shape. The blue cluster does not have any overshoot and a short wavelength, as well as a high SNR, while the red and green clusters show distinct features of an action potential.

mean ISI, by considering ISI values below the mean ISI. Successive intervals below the mean of this redistribution are then counted as bursts. This method is chosen because it requires no parameters and is theoretically very suited to handle various types of bursts by adapting to the statistics of the signals.

Although local field potentials might contribute greatly to quantification of neuronal synchrony and oscillations, only preliminary analysis of these signals has been performed. Results are shown in appendix 5.5.1, but methods for this section were not optimized. Instead, focus was placed on quantifying firing activity in acute slices.

Chapter 4

Results

4.1 Clinical procedure and slicing

A total of 31 animals was used. Table 4.1 shows that 5 control animals, as well as 2 6-OHDA animals could not be used. Two 6-OHDA animals died directly after injection, displaying erratic behaviour and excessive activity, running in circles around the cage. During autopsy of these animals, blood haemorrhages were observed as dark spots on the lungs, which supports the theory that an overdose of the injection led to hyperactivity and subsequent lung failure. In control animals, several experiments were categorized as failures either due to faults in the measurement setup or due to wrong composition of the medium.

Table 4.1: Overview of animal success rate

Control:	Slicing practise	5
	Successful	12
	Failed experiment	5
6-OHDA:	Successful	7
	Deceased	2
Total		31

Per animal, about 9 to 10 slices of the striatum could be obtained from each hemisphere. After visual inspection of the tissue damage, random slices (between 1.6 and 4.6mm deep, as compared to the Rat Brain Atlas) were selected for each experiment. Success rate (number of active slices) varied among animals, but clear action potentials could be recorded from each animal.

Although 6-OHDA lesions were applied unilaterally, the unlesioned side is considered equal to control conditions. However, both categories are separately included in results.

4.1.1 Protocol verification

During the experiments, the protocol described in 3 was followed as closely as possible. In order to verify that the ACSF solution was as specified, the pH and osmolarity were measured during two experiments. Freshly made aCSF had an osmolarity of 305 mOsmol/kg and a pH of 7.68, while oxygenating resulted in a pH of 7.45. Over the course of 30 minutes without oxygenation, the pH increased to 7.66. In order to continuously monitor pH, phenol-red was added to the medium. However, this could not provide the required resolution to distinguish oxygenated aCSF, so this was left out in later experiments. The temperature in the recording chamber was 33°C at a setpoint of 36°C and using the metal spacer and a flow speed of 1.5mL/min. Using a plastic spacer results in an actual temperature of 27°C.

Due to inactivity of the slices, the protocol described in chapter 3 was adapted to evoke activity in slices that were otherwise inactive. However, changes to the protocol were not carried out consistently over experiments, since each slice reacted differently to the given stimuli. No stimulation protocol was found that could reliably evoke activity in all slices.

In striatal slices, electrical stimulation was applied directly after transferral to the recording chamber, with no observable effect. All active striatal slices were only active following increased mechanical pressure on the mesh. In only 4 striatal slices, electrical stimulation was able to recover activity, while increased mechanical pressure evoked a reaction in 29 slices. In active hippocampal slices, activity was recorded without electrical stimulation or significant mechanical pressure. Increased activity was evoked by applying mechanical pressure.

4.1.2 6-OHDA model verification

5 out of 7 6-OHDA animals showed a clear reaction to the apomorphine challenge. About 2 minutes after injection, these animals started to turn counter-clockwise, while the 2 unaffected animals walked around in the cage with no clear pattern. Additionally, animals were observed to develop a preferred side for walking and moving, clenching their frontal paw during rearing tests. For the animals that did not respond to apomorphine, similar behaviour distinct from control behaviour was identified, and these animals are still considered parkinsonian. Further behavioural tests were not analysed.

4.2 Waveform analysis

Although clear action potentials can be observed on a subset of electrodes, signal-to-noise ratio in acute slices is often very low (for example, see figure 4.1). In the recordings, various sources of noise and artefacts were observed, which result in false threshold crossings. Before analysis of recorded firing rates, it is necessary to reject these waveforms from the data set. As described in the methods, preliminary spike rejection was aimed at rejecting stimulation artefacts and low-amplitude waveforms. However, the overview of collected waveform shapes shows a great variability, which makes automatic classification virtually impossible. Because automatic spike classification was insufficient, additional boundaries were created to semi-manually distinguish noise from signals. Results of noise rejection can be found in appendix B Supervised PCA clustering of cluster templates was performed on normalized templates, and resulting clusters were manually classified.

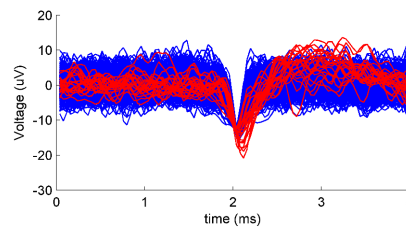


Figure 4.1: Example of recorded waveforms with a low signal to noise ratio.

4.2.1 Analysis of putative noise waveforms

A large fraction of spike clusters that were obtained following spike sorting have waveform shapes that are not typically associated with action potential dynamics (i.e. no overshoot, discontinuities or multiple peaks. In order to better understand whether putative noise clusters are indeed non-physiological, several additional experiments are performed.

Figure B.1 in the appendix shows that the majority of STA templates that have only a negative phase, with no significant overshoot and a timeframe of ~ 0.2 ms. These signals often display regular firing patterns which scale with the threshold value. Although their waveform shape is too indistinct for spike sorting, these waveforms could be the result of neuronal activity and as such be used as a measure for ensemble activity. However, conventional tests on the statistics of these clusters (e.g. looking at ISI and firing rates) cannot be used, since it is impossible to estimate how many neurons are represented in these clusters. If these clusters correspond to physiological signals, they should react to pharmacological and/or electrical stimulation. However, no reaction to such stimulation was observed in any of the evaluated slices.

The most likely origin of the monophasic action potentials is bias of the spike threshold. Too low threshold values result in non-physiological noise spikes being recorded. This is shown by the fact that the number of detected spikes and threshold value are correlated, as seen in figure 4.2, while the waveform shape stays the same. In fact, linear fitting at detection rates until 5 (the threshold where noise is no longer detected) results in $R^2 = 0.999$. At higher thresholds, the signal is no longer dependent on the threshold and deviates from this linear correlation.

Introduction of extra noise by lowering of the threshold does not change the shape of the spike triggered average, hence it is impossible to distinguish whether these signals are signal or noise. However, higher threshold values reveal that there are indeed different waveform shapes that do show a significant overshoot. In cases where the threshold was set too low, these signals will be masked by the noise waveforms.

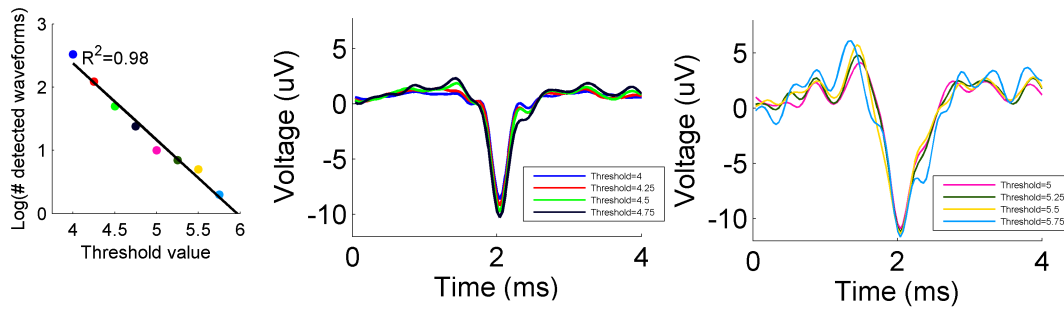


Figure 4.2: Detection rates and resulting STA for different threshold values. Noise detection rates logarithmically correlates with threshold value, and waveform shape is monophasic. Higher threshold settings reveal that 'real signals' do have an overshoot.

Although these monophasic waveforms are considered noise, it seems odd that the shape is constantly negative. This is a bias resulting from the negative threshold, which only records spikes with a negative slope and hence rejects all similar positive noise. This is shown by recording filtered electrode data and redetecting spikes with both a negative and a positive threshold. Resulting clusters showed as many positive as negative spikes and had an average baseline waveform shape (figure 4.3). If these signals represented action potentials, then the average should have been more distinct (as seen in the figure).

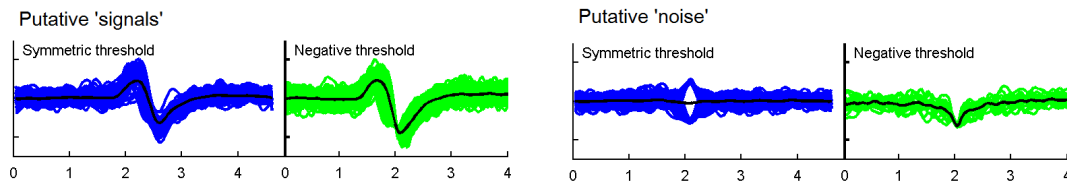


Figure 4.3: *Left*) Experiment using both a positive and negative threshold, or just using a negative threshold. Putative action potentials will result in a significant deviation from baseline, because their shape is deterministic. Putative noise waveforms will average to zero due to their random shapes. *Right*) Overlay of waveforms shows noise and signal are hardly distinguishable. The overshoot of the signal does not exceed noise levels, while the amplitude of noise and signal are also equal.

4.2.2 Action potential characteristics

Following the semi-manual classification of noise and signal, the data set of accepted waveforms is significantly reduced. Of the 7673 cluster templates, 71% was rejected as noise. Figure 4.4 shows the waveforms of clusters that were accepted as physiological signals, as distinguished by peak-valley distance. Clear distinctions can be made in the wavelength and shape of the different signal types. Due to underclustering in the spike sorting algorithm, multiple clusters can represent a single source. Resulting clusters are therefore grouped per electrode and neuronal type.

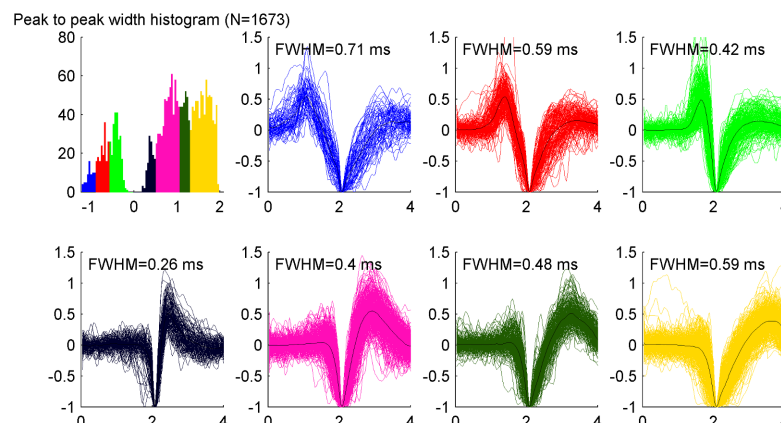


Figure 4.4: Accepted cluster waveform shapes (normalized amplitudes). Top left: a histogram of valley-to-peak width is used to cluster similar waveform shapes.

Based on the waveform shapes, (groups 1-3) of recorded neurons displays a peak before the negative slope that is higher than the overshoot phase. This corresponds to the waveform shapes of putative cholinergic interneurons (see figure 2.4). Group 4 clusters show much faster dynamics which stereotype fast spiking interneurons. However, the vast majority of waveforms shows a slow and high overshoot which is characteristic of the medium spiny neuron (groups 5-7).

Distribution of neuronal signals

In further analysis, clusters were recorded from a total of 53 slices from 3 control and 7 PD animals. These experiments were carried out using the same protocol. Previous control experiments were considered only to illustrate examples, not for statistics. Of the viable slices, 8 (4 unlesioned, 4 lesioned) showed activity in both the striatum and hippocampus, while 12 experiments recorded activity from the hippocampus in slices where the striatum was inactive. Recordings from striatum and hippocampus of the same slice are regarded as independent recordings.

Table 4.2 shows the distribution of waveform types between striatum and hippocampus. Interestingly, all waveform types can be found in both structures.

Table 4.2: Distribution of waveform types for striatum and hippocampus

Neuronal type	1	2	3	4	5	6	7
Striatum (N=1068)	2.34	8.71	11.80	7.68	27.15	14.12	28.09
Hippocampus (N=297)	8.42	5.39	7.74	1.35	11.11	19.19	46.80

4.3 Recorded amplitudes and active channels

Figure 4.5 shows the distribution of recorded amplitudes per cluster and number of active channels as recorded in different brain regions of control and lesioned animals. Amplitudes are typically around $20\mu\text{V}$, with higher amplitudes being recorded in individual cases. Data ranges of amplitudes are similar across animal groups and brain area's.

Additionally, the number of active channels is very low for all recordings, around 10. For extremely active slices, about 20 to 30 active channels can be found. Although the success rate for slices in the hippocampus is much higher, the number of active channels is still relatively low.

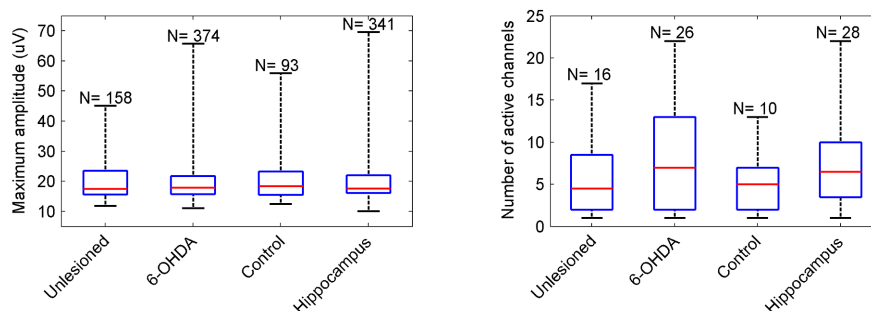


Figure 4.5: Top: box plot of the distribution of absolute amplitudes recorded from acute slices. Bottom: distribution of number of active channels per slice. Whiskers of the boxes indicate the maxima of the data range.

4.4 The striatum is not spontaneously active

In order to record spontaneous action potentials, slices are allowed to equilibrate after transferring to the recording chamber. However, to avoid including dead slices, the activity of a slice is monitored immediately after transferral. This is done by inspecting visually the waveforms that are detected. In general, this process was trivial; for active slices, clear and stable waveform shapes well above threshold could be detected on a subset of electrodes. However, in many cases these action potentials quickly subsided after several minutes and did not return within 30 minutes after transferral. During the periods of activity, the amplitude of the action potentials stays the same, but the frequency gradually goes down until no more activity is observed.

Several tests were performed on slices to determine whether slices were still active after the bursts subsided. Following mechanical pressure, electrical stimulation was applied to evoke action potentials. In several cases (N=4), these stimulation trains were successful in returning action potentials. However, shortly after stimulation the activity would fall silent again.

Pharmacological stimulation using L-glutamine was applied in 10 slices, but was not observed to have any effect. Additionally, inhibition of FSI's using IEM-1460 was applied in 5 slices but also did not result in increased activity.

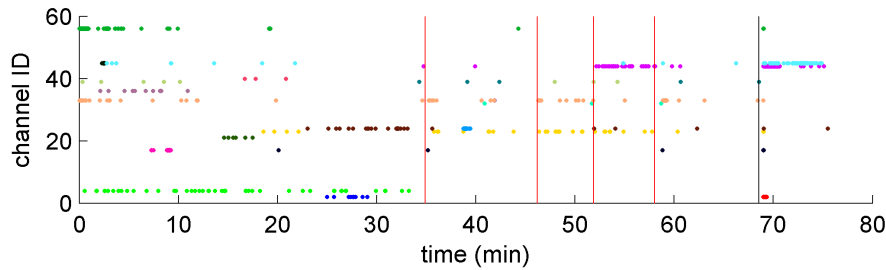


Figure 4.6: Example recording where electrical stimulation was applied in a relatively active slice. Red lines indicate time of stimulation trains. Following stimulation, previously silent channels record activity again (e.g. channel 33 at 34 minutes, channel 44 at 52 minutes). Black line indicates application of mechanical pressure, which further activates channels.

4.5 Hippocampus provides positive control

In order to show that inactive slices were not dead, 28 slices were used to also record from the hippocampus. When activity could not or no longer be measured in the striatum, the mesh was gently lifted and the slice was shifted so that part of the hippocampus and surrounding area covered the MEA. Results of these experiments are shown in figure 4.7. In 24 out of 28 slices, activity could be recorded in the hippocampus, the other 4 slices were severely damaged. However, the striatum was not or hardly active in 16/28 slices. Furthermore, in contrast with recordings from the striatum, action potentials from the hippocampus could be detected without substantially pressing the slice, and typically persisted over extended times. However the number of active electrodes was similar to that of the striatum.

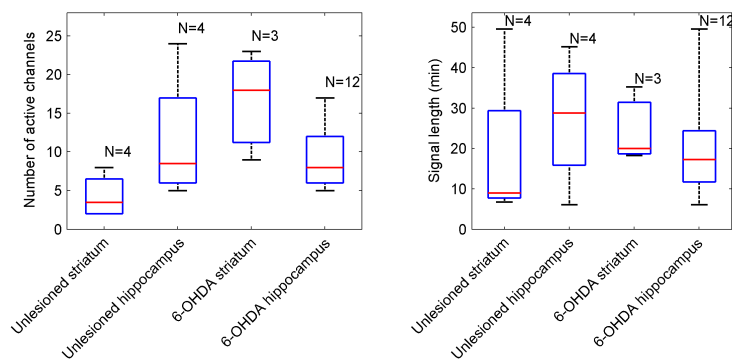


Figure 4.7: Box plots of the number of electrodes and signal length (maximum time at which activity was still recorded) of the recorded signals from the striatum and hippocampus of the same slice.

In 6 recordings of the hippocampus, addition of L-glutamine (direct application) to the medium resulted in significant increases in activity. After application of higher doses of glutamine, firing rates increased and activity was recorded on previously inactive electrodes. If too much glutamine was added, the activity declined after a period of high-frequency firing, as shown in figure 4.8. This shows that there is sufficient diffusion of chemicals from the medium to reach the active neurons and manipulate their activity.

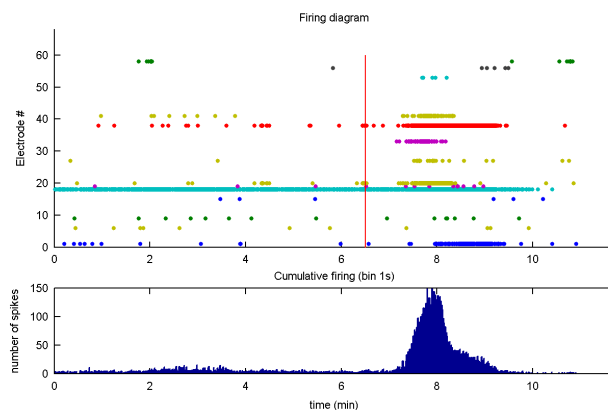


Figure 4.8: Top: raster plot of activity recorded in the hippocampus before and after application of glutamine. Below: histogram of number of waveforms recorded every second, as summed over all electrodes.

4.6 Quantitative analysis of firing patterns

The distribution of analysed firing patterns is shown below. As can be seen, a large fraction cannot be analysed because there are not enough spikes to construct the discharge density histogram. Furthermore, almost all putative neurons are classified either as 'bursty' or 'random'. The few neurons that were classified as regular did not actually show regular behaviour, but rather consisted of only one burst which had consistent ISI values.

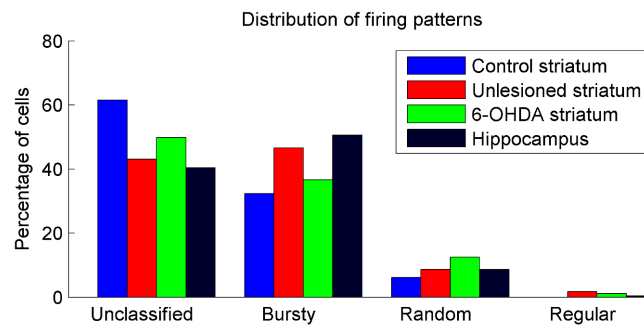


Figure 4.9: Distribution of firing patterns, as determined using the discharge density histogram.

Burst characteristics were collected for all signals, but visual identification of the results showed that due to the high heterogeneity of signals, burst identification failed. Hence, this analysis was left out of analysis.

Figure shows the distributions of frequencies in spikes/minute for the different slice types, with empty spike counts left out. Empty spike counts make up 40%-45% of the recorded time. In addition, the cumulative bins show that 60% of spike counts are less than 8 spikes per minute, while 90% contains less than 60 spikes per minute. Interestingly, slice types show slight peaks between 10 and 20 peaks per minute, especially striatal slices.

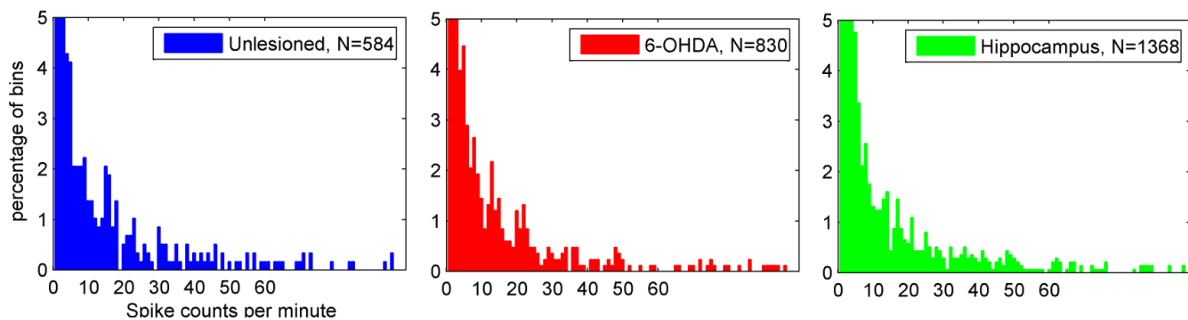


Figure 4.10: Histogram of spike counts (bin size = 1 minute) per slice type. Bins with 0 spike counts are not included, but would respectively add 85, 77 and 59%. Although not shown here, the tails of the distribution reach 3373 spikes/min.

Chapter 5

Discussion

Hypotheses about the activity in striatal slices formulated that there should be a difference between firing rates in parkinsonian and healthy animals. Furthermore, blocking of fast spiking interneurons was expected to result in higher firing rates and increased number of bursts in the parkinsonian striatum. The presented results fail to provide proof for these theories, as no significant differences could be found in the firing rates recorded in the striatum. Spontaneous activity was too low to adequately quantify neuronal activity. In addition, activity induced by mechanical pressure, electrical stimulation and drug application effectively masks the characteristics of spontaneous activity. Because activity was so low, no clear conclusions can be drawn regarding the hypotheses.

Considering that very little activity was recorded in the majority of slices, the question arises whether the methods used here are valid, or whether technical factors have contributed mostly to low recorded activity. Here, a discussion regarding method validity and technical issues is presented. Firstly the positive control experiments in the hippocampus are discussed and compared to literature. Various steps in the protocol are highlighted that may contribute to cell silence. Additionally, physiological origins of the slice inactivity are critically reviewed and backed up with additional literature.

The fundamental conclusions arising from this discussion have significant implications for future research in acute slices of the striatum. Several requirements and strategies are presented that should enable further investigation of FSI's in acute slices. This chapter concludes by providing recommendations for future work and improvements that should be applied to the setup and analysis.

5.1 Validation of setup: hippocampal slices

Control experiments in the hippocampus have been partially successful to show that spontaneous activity can be recorded using the MEA setup. While firing patterns are similarly sparse like in the striatum (number of active channels), this activity was picked up without mechanical pressure or electrical stimulation. Furthermore, spontaneous activity could be recorded for over 60 minutes, indicating that medium composition is sufficient to facilitate sustained activity.

Although hippocampal slices are often used for studying or synaptic plasticity in Schaffer collaterals, few quantitative reports on spontaneous firing rates were found. Firing rates previously recorded in hippocampal slices range from 1.5 to 5HZ [125], although many different spontaneous LFP waves have been reported. These waves often produce subthreshold fluctuations in membrane potentials, and accompanying action potentials are not reported. Although protocols for slice preparation were followed closely from protocols for hippocampal slices, activity is less reliable and widespread than reported in literature. Several technical factors can contribute to this.

Because the slice was oriented to preserve the striatal connections, hippocampal connections, which typically lie in the transverse plane, might be severed. In the transverse slices of the hippocampus, only one slice was successfully recorded on 15 active channels for over an hour. Furthermore, due to the position of the hippocampus in the dorsal part of the brain, the tissue there was often damaged by shear stress. The blade could not always slice perfectly through the tissue where ventricles are present. Glue sometimes stuck to the brains, and extra pressure was required to release the cut slices. Lastly, the hippocampus has a very anisotropic shape which is unevenly distributed among slices. This leads to higher variability of the slices and poorer tissue quality. Using transverse hippocampal slices, spontaneous activity was recorded for longer duration in one slice, but activity in this slice showed similarly sparse spike counts as in other slices.

Despite the aforementioned deprecation of hippocampal slice quality, it was possible to record from this area for longer durations and with greater success than the striatum. Because slice quality of the hippocampus is compromised, it is not possible to record relevant network activity. Nevertheless, the experiments in the hippocampus serve as a verification that slices of the striatum are typically not dead, but rather inactive. These experiments also show that the technical setup and protocol are capable of recording sufficiently from acute slices, but that slice preparations are not in optimal condition.

5.2 Technical factors in slice inactivity

There can be several reasons why so little activity can be measured in a slice. Technical issues during experiments can prevent any action potentials from being measured, either because the cells didn't survive the procedure or because of errors in the measurement setup. Alternatively, physiological issues could result in cell inactivity. Here several factors that contribute to cell inactivity are discussed.

5.2.1 Protocol

Tissue preparation

Although success rates of experiments on acute slices depend heavily on the quality of the slices and hence on the quality of the clinical methods, several tests have been performed to exclude influences of the slice preparation process. Medium composition, pH and temperature have all been verified. The procedure of brain extraction and slicing was done as carefully as possible and with as few delays as possible to prevent hypoxia and stress. When compared to video journals of similar experiments [126, 127], the time between decapitation and brain extraction was sometimes longer (due to hardening of the skull in aged animals). However, in typical experiments on hippocampal slices, additional dissection is required to extract the hippocampus. This leads to longer exposure times where the brain is deprived of oxygen and ATP. For the striatal slices such additional procedures were not necessary, and oxidative stress should have been minimal. Furthermore, slices were allowed to equilibrate for up to 4 hours before the experiment, which should also increase cell survival of the slices compared to similar experiments.

Mechanical pressure

During the experiments, the slice is pressed against the MEA by using a micromanipulator. As a result, mechanical pressure could potentially lead to membrane rupture and cell death. However, not applying pressure leads to bad contacts, and activity is often only observed after pressing the slice down. Results clearly show that, following mechanical pressure, cells start to fire in high frequency, but eventually become silent again. These bursts are sustained over as long as 5 minutes, indicating that this activity is not detrimental to the cells. Furthermore, the activity can in some cases be elicited by post-pressure electrical stimulation (figure 4.6), indicating that cells are still alive. Additionally, the successful experiments in the hippocampus provide further evidence that mechanical pressure is not responsible for silence in the striatum.

Diffusion of chemicals

In order for cells to survive in acute slices, sufficient supply of nutrients is required. Since the active cells are not located at the surface of the slice, these nutrients must diffuse through the slice in order to reach the cells. If the diffusion is not high enough, this could result in nutrient depletion, which could result in anoxic depolarization. When there is insufficient ATP, sodium/potassium pumps will have insufficient energy to maintain the concentration gradients, and ions will flow out of the membrane, resulting in a temporarily increased potential. However, in the results, bursting activity clearly shows the repolarizing current, which indicates that cells have enough energy. Additionally, the reaction of hippocampal neurons to glutamine 4.5 shows that diffusion through the slice is not significantly hindered.

Cell electrode contact

Despite the use of 3D platinum electrodes on the multielectrode array, recorded amplitudes are lower than reported in previous experiments using the same setup [128]. A possible reason would be damage to or dirt on the electrodes, but impedance of the electrodes was measured to be in the specified range and the conical shape was verified under a microscope. Nevertheless, signal strength was often below the noise threshold. Additionally, the number of active channels was very low, even in hippocampal slices. In the striatum, this can be explained by the organization of neurons in 'patches' of neurons embedded in a matrix which makes up about 85% of the striatal volume [129]. However, in the hippocampus the neuronal density is much higher, especially in CA1 and CA3 regions. This should have resulted in more active channels, provided that the quality of the tissue is ensured. In the consecutive experiments on striatum and hippocampus, the quality of the hippocampus was far from optimal, due to mechanical pressure during striatal recordings as well as shear stress during slicing. Due to the damage and position of the hippocampus, it was harder to accurately place this structure on the MEA. These factors may explain why contacts in the hippocampus were not significantly better than in the striatum.

In healthy hippocampal slices, activity was reported on many electrodes of similar MEA recordings [107]. Because the presented results do not show as high success rates as reported in literature, this may indicate that the cell survival is too low due to errors in the protocol execution. This should be tested by applying a live-dead assay, as discussed in section 5.6.

5.3 Physiological origins of cell silence

Although technical issues seriously affect recorded activity, several experiments have shown that these issues are not essential for recording activity from acute slices. Specifically, the relative success of experiments on the hippocampus has shown that activity in acute slices can be measured and stimulated by applying chemical agonists to the medium. However, experiments on the striatum have not succeeded in providing similar results. This indicates that cells in the striatum might be too inactive to measure spontaneous activity on a MEA.

As described in the theory, the dominant GABAergic currents result in a hyperpolarized resting membrane potential. However, excitatory input from the cortex was expected to lead to activation of the striatal network. The absence of activity could be a result of damage to the corticostriatal synapses, which could be severed during the slicing. Interestingly, the parasagittal plane at $10 \pm 2^\circ$ was reported to leave intact projections of all the basal ganglia structures, including the input from the cortex [100]. Nevertheless, excitatory input is not sufficient, and it is possible that although individual axons are intact more global input is required, but absent in the striatum.

Wilson *et al* have reported that spontaneous activity in striatal slices could not be elicited without pharmacological stimulation [130]. Variation of *in-vivo* recorded firing rates was considerable, while other intracellular experiments in slices did not produce spontaneous activity [131]. However, results provided by Gittis and colleagues show that cholinergic interneurons fire spontaneously at 1.5Hz, even in acute slices. No data for spontaneous activity of MSN's or FSI's was given in acute slices, but *in-vivo*, firing rates of MSN's were typically 1.5Hz, while FSI's fired at rates of 15Hz.

Conversely, recordings from organotypic slice cultures of striatum and cortex show that spontaneous activity of MSN's can be very sparse, with interspike and interburst intervals of 10 seconds [132]. Such random spontaneous activity was also previously reported in the mouse striatum using similar methods as used here. Dehorter and colleagues studied activity in both whole-brain slices and input-deprived striatum, and found sparse single spiking activity in both types [110]. Interestingly, they report that 6-OHDA lesioned animals also exhibited bursts. These recordings were possible in both whole-brain slices as well as isolated striatal slices. This would indicate that afferents from the cortex would not be required to elicit spontaneous activity in the 6-OHDA lesioned animal. However, these bursts could not be reliably observed in the experiments, and a personal communication indicated that the depolarizing agent 4-aminopyridine was used to elicit more activity.

In-vivo, MSN activity is characterized by a cycle of a hyperpolarized DOWN-state around $-80\mu\text{V}$, intermitted by a depolarized UP-state around $-55\mu\text{V}$. In the UP-state, it is possible for action potentials to occur, although GABAergic currents quickly repolarize MSN's to their resting state. This cycle is seen both *in-vivo* [130, 133–135] and in organotypic slice cultures [99], and occurs at frequencies around 1 Hz [134]. In contrast, MSN's in acute slices do not transition into an UP-state [136], presumably due to the lack of cortical input. However, evidence for depolarizing currents are observed in intracellular measurements [110], but these are generated inside the striatum and do not result in generation of action potentials.

Following these previously reported results, it can be concluded that activity in the striatum requires strong external input which cannot readily be spontaneously provided in acute slices. *In-vivo* the cortex is much more active, whereas slicing can result in severed corticostriatal connections which reduces striatal excitation. Since there is a high degree of convergence from the cortex to the striatum [137, 138], part of this input may be severed during slicing. This would then not be enough to provide the excitation required for sustained striatal activity. An alternative explanation for the lack of oscillating behaviour is that such activity requires much higher energy consumption, which may not be appropriately facilitated by the aCSF composition. Khurana and Li indicate that glucose and oxygen supply alone is not sufficient for satisfying energy needs in the slices, and suggest addition of lactate and other nucleotides to promote and facilitate high energy metabolism [139].

5.3.1 Recovering cortical input

Remarkably, it was reported that following slicing preparation, incubated slices of the nucleus accumbens (the ventral striatum) were able to regain their cycling behaviour after one day *in-vitro* [140]. Coronal slices were incubated in Neurobasal-A medium, a growth medium which is normally used for cell cultures. After respectively 6 and 24 hours of incubation, cells started firing in bursts and exhibited downstate-upstate cycling, as measured intracellularly figure 5.1. Conversely, slices that were incubated for 1 hour did not show any upstate activity. Additional measurements were performed to verify that glutamatergic input was driving the UP-state, EPSP's were increased while no postsynaptic plasticity was observed. In this project, equilibration time was over an hour, but no spontaneous activity was

recorded. However, it was subjectively observed that recordings more than 4 hours after slice preparation tended to be more successful, which could indicate that this UP-state recovery may also occur in the striatum.

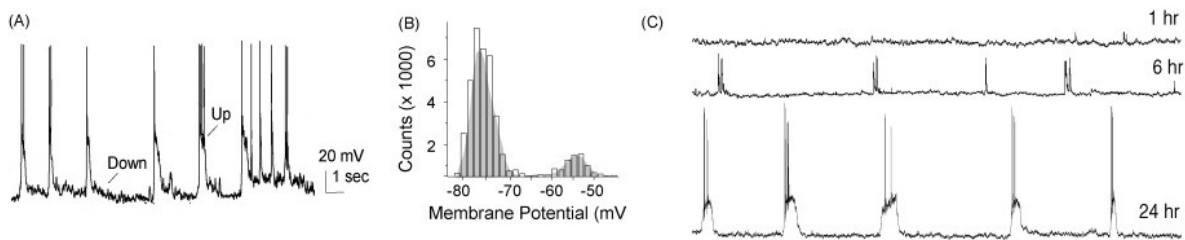


Figure 5.1: Evidence that UP-state can be recovered in the nucleus accumbens following short-term culturing, as adapted from [140]. A) Example of intracellularly recorded spontaneous activity showing UP-states in the membrane potential, during which action potentials can occur. B) Histogram of the recorded potentials shows a bimodal distribution. C) UP states only occur following 24 hours of incubation. After 6 hours, depolarizing bursts are observed, but these are not persistent and do not facilitate action potentials. It is theorized that this is the first stage of homeostatic recovery of the UP-state.

In this project, although glutamatergic input seemed to be lost following slice preparation, the effect of cortical input was simulated by applying L-glutamine and electrical stimulation. However, these methods failed to provide significant firing rate increases in the striatum. Parameters of these experiments were not optimized (i.e. stimulation frequency and glutamine concentrations were low, which only resulted in temporary increases. In order to reliably and consistently elicit activity, permanent stimulation should be applied at physiologically relevant frequencies and concentrations, since 'jump-starting' the network did not produce the desired effect.

5.4 Analysis of quantitative results

Although slices were highly inactive, several results have been obtained from striatal and hippocampal slices. Waveform shapes have been identified and firing patterns have been presented for different slice preparations. Here, the value of these results is discussed.

It should be noted that the experiments were mostly focused on characterizing whether the setup was capable of recording action potentials from the striatum. As such, there is a lot of variation among experiments, and sample sizes for experiments with similar conditions are very low.

5.4.1 Characteristics of recorded signals

The waveform shapes of accepted spikes largely reflect those reported in literature [67, 77]. Medium spiny neurons were reported to have slow waveforms, with peak to valley times of 560 to 1500 μ s. FSI's on the other hand have much shorter wavelengths, as identified in the results. Interestingly, no stable signals corresponding to cholinergic interneurons were recorded. Signals that have waveform shapes corresponding to these interneurons were not spontaneously active, and could not be classified as regularly firing.

However, these waveform shapes are not unique to the striatum; hippocampal slices show similar waveform shapes. Furthermore, it has been shown that waveform shape is strongly dependent on the relative location of the electrode with respect to the cell body [141]. This makes identification of cell types based on waveform shape very inaccurate, and it may be impossible to distinguish whether signals are recorded from the striatum or from neighbouring nuclei. Instead, a microscope should be used to more accurately place the striatum on the MEA and exclude electrodes recording outside the striatum.

Significance of activity quantification

The firing rates reported here are very sparse (less than once per minute) and random. Although firing rates and patterns have been identified in active slices, these results are heavily influenced by external manipulations. Because the activity was so low in general, most attention has been aimed at finding out how the activity is affected by external factors. To this end, slices were pressed, stimulated and chemically manipulated during experiments. As a result, recorded activity does not reflect spontaneous activity that is normally seen *in-vivo*. More importantly, when no activity change was found after stimulation, different forms of stimulation were applied. This restricts any analysis of spike patterns, because it is not known how exactly this activity was evoked. This means that conventional measures of activity and neuronal classification such as discharge density, firing rate and burst patterns cannot be compared with literature, and quantitative analysis cannot yield significant results.

5.4.2 Obstacles in data analysis

Although clear action potentials can be recorded on the setup, the data analysis is impeded by the false detection rates due to errors in the threshold setting. In order to handle the large datasets and to provide more objective analysis, an automatic algorithm was designed. However, the many sources of variation between recordings complicate automatic data analysis and can result in significant bias of the presented results. Most of the complications in data analysis were caused by the low amplitude of recorded waveforms and the low signal-to-noise ratio.

In order to distinguish action potentials from different sources, the PCA-based spike sorter attempts to find the vectors that provide optimal distinction between groups of similar waveforms. However, the false positive waveforms resulting from the low threshold impede spike clustering. Since the number of noise waveforms is much higher than the number of signal waveforms, this will form a large cluster. Differences between signals from two different sources are masked by the difference between signal and noise, leading to false outlier rejection of signal waveforms.

The PCA clustering scheme is also ill-suited to handle bursting neurons. During bursts, the amplitude of recorded waveforms decreases over time. This causes a gradient in the waveform shape, which cannot be resolved in the PCA space. Here the differences between signal and noise are masked by the differences among waveforms in a burst. As a result, the waveforms are represented using non-ideal principal components as a single, elongated cluster. Depending on the ratio of signal and noise, this can either result in inclusion of noise in the cluster, or in false rejection of the cluster due to changes in the STA.

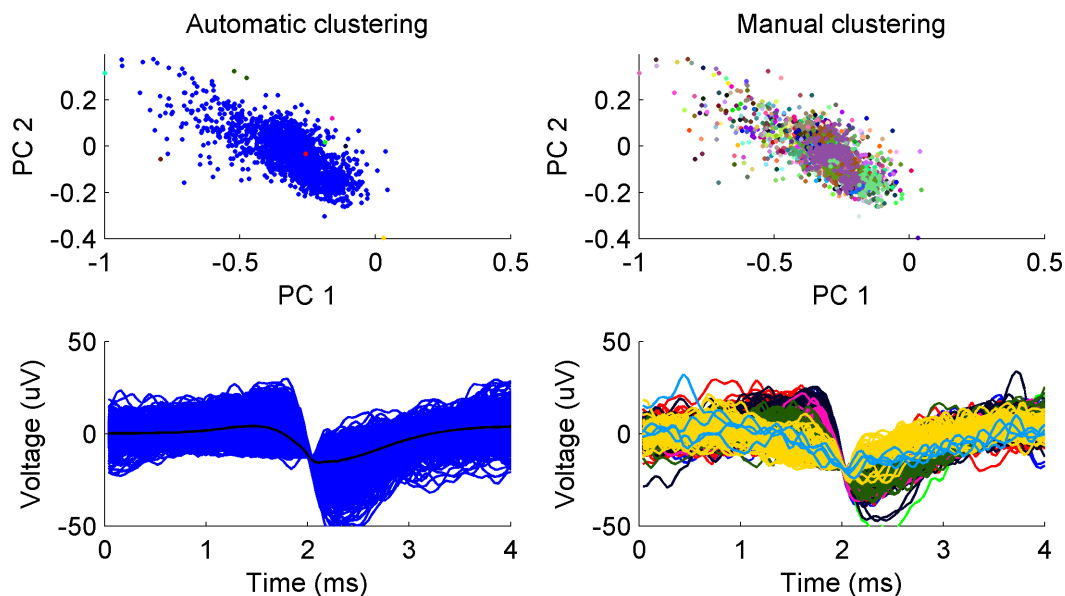


Figure 5.2: Failed PCA clustering due to bursts. In a burst, the amplitude and shape of waveforms may differ, resulting in a gradient in the PCA representation. Consequently, density-based clustering accepts all waveforms as part of the cluster. This significantly changes the STA, which is used for selection of physiological signals. Manual underclustering shows that distinct waveform shapes are possible, and that noise waveforms are also included in the accepted signals.

Because noise waveforms make up a large fraction of recorded waveforms, automatic sorting of signals was severely interrupted. Underclustering was used as a method to distinguish noise from signals, but this resulted in many clusters coming from the same source. Identification of noise clusters was required to determine a data set of clusters that could be accepted as physiological waveforms. Due to the variability among noise cluster waveform shapes, automatic classification was made impossible. To resolve differences in signal amplitude between electrodes and compare averaged waveform shapes, the signals were normalized to their maximum amplitude. However, this greatly increases noise representation in the waveform, leading to variability between templates. Conventional classifiers such as the FWHM or peak-to-valley did not always have a significant meaning when templates were corrupted with additional peaks. It should be noted that these peaks in some cases can also be caused when spikes from two neighbouring neurons occur almost simultaneously. Although these spikes are physiological, they cannot be adequately analysed and should also be discarded.

As a result, the data analysis is heavily influenced by the experimenter. In order to reduce the arbitration, an extensive deliberation was performed to verify that monophasic clusters did not represent signal waveforms. This has shown that significant bias is introduced by using a negative threshold, and that errors in threshold value lead to high false detect ratio's.

5.5 Implications of results

Although the hypotheses of this project could not be adequately tested in acute striatal slices, the results presented here have some significant implications for future work on acute slices in general, and on the investigation of beta-oscillations in the striatum.

Although the microelectrode array is capable of recording from over 60 sites, the low probability of cell contact does not allow for extensive network-wide recordings of the striatal cells. In the presented results, about 5 to 10 electrodes were active for a viable slice, but no quantification of the contacts with silent cells can be made. This means that activity of single cells may not reflect the true network dynamics under investigation, because it is not clear what the relative sample size from the total population of active neurons is.

5.5.1 Can FSI blocking be evaluated in acute slices?

Acute slices theoretically provide a better simulation of the morphology of the *in-vivo* brain structures than cultures do. However, the current results raise questions on whether signalling in the striatum is also more realistic and whether it can reflect the actual network dynamics of the basal ganglia with sufficient accuracy. In order to obtain a more stable and controlled experiment on striatal slices, activity should be enhanced through electrical or pharmacological stimulation. However, in this way the network activity will no longer be fully determined by the underlying dynamics, but instead might be dictated by the artificial stimuli.

Extra care should be taken to prevent suppression of the network dynamics by external stimulation, as this is also the mechanism assumed to underlie deep brain stimulation. Current understanding of DBS is that the original firing patterns are suppressed by stimulation [96]. Mimicking of cortical activation might result in very similar behaviour, and this effect should be appreciated when analysing the effect of bath-applied drugs.

In order to measure the effect of the FSI inhibitor IEM-1460, glutamatergic input from the cortex is required, because Glu-receptors are the target of this blocker. Electrical stimulation should therefore target cortical cells and not striatal cells, because glutamate release is required for the blocker to be effective. To achieve this, the slice should be positioned on the MEA in a way that both the cortex and striatum are accessible. This requires more exact placement of the slice. For this purpose the MEA should be placed under a microscope, and careful note should be taken as to which electrode records from which region in the slice. This will lead to even less channels being available to record from the striatum. To tackle this, different electrode layouts (rectangular versus square) may be more beneficial for these experiments.

Optogenetics

As an alternative to electrical and pharmacological stimulation, the employment of optogenetics [142] might provide a means to selectively inhibit or excite specific cell types in the striatum. This technique is based on genetical manipulation of neurons, which makes them sensitive to light. Specific proteins such as channelrhodopsins or halorhodopsin can be expressed in neurons by transfection (for example viral transfection). These proteins are sensitive to light of a specific frequency and behave as light-dependent membrane channels. When stimulated optically, these channels open up, which depolarizes (channelrhodopsin are sodium and potassium permeable) or hyperpolarizes (halorhodopsins are permeable to Cl^-) the stimulated neuron. Channels close within milliseconds, which gives this method high temporal resolution. Since protein channels can be selectively transfected to one cell type, the experimenter can exert a powerful control over neuronal activity. In the striatum, this technique has already been employed to target FSI's [80] as well as indirect and direct pathway MSN's [143]. This technique could be used to simultaneously simulate cortical input and block FSI's, providing an elegant solution to the problems encountered in this project.

Local field potentials

Although action potentials in the striatum are sparse, cortical activity may still depolarize MSN's. This might instead be measured in the local field potential. Simultaneous depolarizations of the MSN population may be summed and could show in the LFP. Typically, synchrony and oscillations should be seen in LFP recordings, since synchronous subthreshold depolarizations of a neuronal ensemble have been previously reported. Even when glutamatergic input is insufficient to initiate action potentials, intact corticostriatal connections should result in depolarizations that might be picked up in LFP's.

In this project, local field potentials were occasionally recorded in active slices and preliminary analysis was performed (see appendix), but no clear indication of synchrony could be found. Even when clear action potentials were recorded simultaneously, no correlation with local field potentials could be found, and periodograms only showed noise footprints. Further analysis of LFP's is warranted before drawing conclusions on their value, but it should be noted that in order to evaluate oscillations and synchrony, the local field potential should be preferred over analysis of action potentials.

5.6 Recommendations

5.6.1 Improving slice quality

In order to improve work on acute slices on microelectrode arrays, several focus points can be distinguished. An important part of these experiments is that the slices are in optimal condition. To achieve this, slicing experiments were as close to previously reported methods as possible, but errors in slice handling can never be completely avoided. Nevertheless several steps may be taken to increase cell survival.

- **Shear stress during slicing**

As mentioned the slicing of brain tissue is a delicate task which requires intervention of the investigator to prevent shear stress in the brain and to prevent the slice from folding around the blade. This is done by carefully holding the slice in place with a brush, which might cause damage to the tissue. Additionally, an agar block was placed behind the brain reduce shear stress, but this was not optimal and sideward stress could not be prevented. Additionally, chemical reactions of the glue in ACSF sometimes hindered slicing. In order to overcome these problems, the brain could be placed in an agar block which immobilizes the brain and maintains its structure during slicing, as suggested by [144].

- **Slice incubation**

The equilibration of slices in the waterbath should be improved by creating a different method of bubbling carbogen through the medium. Temperature in the medium cannot aptly be regulated to 36° because of the indirect temperature control and outward convection. Incubating the slices could increase viability and might also enable experiments over more than one day [145]. Reduced time constraints would allow the investigator to take more time to carefully investigate all available slices. As previously discussed, striatal slices might benefit particularly from longer incubation, since the glutamatergic state cycles may be restored

- **Slicing temperature**

Work on slices of the cerebellum has suggested that slicing at physiological temperatures rather than ice-cold aCSF might be beneficial to tissue survival, especially in older animals [146]. This would be especially relevant for 6-OHDA animals, which are generally more than 2 months old at the time of the experiment.

- **ACSF composition**

The composition of ACSF as used here is according to conventional protocols for brain slices. However, different methods have shown that in order to obtain higher quality slices and to further prevent ischemic damage, several adjustments might be made. Because there are many different medium compositions which may have only slight advantages over one another, an optimization of aCSF composition would be too ineffective. Nevertheless, two possible variations that might be of specific use to this project can be distinguished. The addition of lactate, which is required for intense neuronal activity [147] might be required for generation of oscillations in the cortex, and as such provide better input to the striatum. Additionally, better protection during slicing might be obtained by replacing NaCl with glycerol [148] or by adding HEPES to prevent enema [149].

An extensive review by Khurana and Li highlights various sources of cell degradation as a result of the slicing and incubation protocol [139]. Although conventional slicing methods, which have been adopted here, are widely used for a variety of tissue types, it is postulated that oxygen partial pressure required for slices to stay alive may need to be much higher than previously thought. Additionally, they make an argument for further investigation of in-vivo energy and nutrient consumption to provide a better suited environment that can facilitate different activity states, in order to better simulate in-vivo activity in acute slices.

5.6.2 Evaluating slice quality

Because the neural tissue is sensitive to mechanical manipulation and stress, the quality of each individual slice remains uncertain. Considering the limitations on the time frame of an experiment, a quick decision needs to be made about whether to continue recording from a slice. However, discarding slices based on spontaneous activity will bias the results and result in very low success rates. In order to obtain statistically significant results, this would require a disproportionate number of animals. Instead, efforts should be focused on characterising and improving cell survival in the slices. Additionally, quick viability checks should be developed, possibly by adding a depolarizing agent or by optimizing stimulation protocols.

Although the measures mentioned above might contribute to slice quality and experiment success rates, it is necessary to create a set of assessments of slice quality to ensure that slices are appropriate and valid. In the experiments of this project, slice viability was tested by stimulating electrically and pharmacologically, as well as examining other brain areas of the same slice. However, clearer and more systematic verification methods of cell survival, such as live/dead assays, would be highly recommended. In [145], such assays are implemented by incubating slices with a fluorescent marker propidium iodide and DAPI to find the ratio of live and dead cells. Alternatively, stronger depolarizing agents than glutamine could be added to the medium to evoke activity that can be detected. As shown in [110], 4-aminopyridine opens up sodium channels, leading to increased activity, even in the relatively silent striatum. Alternatively, high potassium concentrations are typically used to ensure activity [150, 151]. However, application of such chemicals will lead to changes in network activity that should be accounted for. Activity should be allowed to settle before recording of spontaneous activity is possible.

5.6.3 Improving measurement setup

In addition to improving cell survival, several improvements can be made to the recording setup.

- The cell-electrode contact could be improved by coating the MEA with adhesives, such as polyethyleneimine, which is also used for cell cultures, and was used in the original paper presenting the 3D-MEA [107].
- The temperature control of the MEA setup could be improved by reducing convection to the environment, which at 21° takes up a lot of the heating power. Additionally, steps should be taken to prevent oxygen and CO₂ from escaping the aCSF, for example by putting a lid on the MEA chamber. Furthermore, the custom conductive plate between heating element and MEA chip was too thin, which resulted in poor pin contact between the headstage and the chip and subsequently increased noise levels.
- The mesh that was used consisted of a simple ring with a nylon mesh glued to it. However, the mesh was not optimally fitted to the MEA area; applying too much pressure led to sideways movement and contact loss. This could be improved upon when performing future experiments.

5.6.4 Improving data analysis

Spike detection

In the presented results, false positives due to noise, stimuli and artefacts made up a large portion of data. Additionally, noise thresholds were often inadequate because the noise was not constant during the course of an experiment. Applying mechanical pressure to improve slice contact inevitably results in changing noise levels and therefore changes the false detect ratio. This required a highly customized noise rejection scheme which is tailored to this particular data set and may not have any practical value for future data sets. These issues could have been solved if a higher threshold was used, but given the low signal-to-noise ratio, this would have led to high false rejection ratios. Instead it would be more suitable to apply a dynamic threshold, which monitors the noise levels and adjusts the threshold automatically. This would result in less false positives and would also improve spike sorting algorithms. It should be noted that for analysis of spike waveforms, inappropriate detection thresholds are detrimental to significance of results as a result of differences in noise levels between electrodes which are exaggerated during data analysis.

Spike detection based on amplitude threshold assumes that signal to noise ratio is very high. Ideally, the threshold should lie exactly between noise level and signal amplitude, so that noise spikes will not be classified as events. However, in the present recordings, signal to noise ratio is often too low, and action potential amplitudes barely reach above noise levels. The value of the threshold now determines how many waveforms are recorded. Choosing a safe threshold which only allows high amplitude waveforms would yield very few signals, and does not suffice to understand network activity. In order to solve for this, SNR should be improved, either by increasing the input impedance of the electrodes or by improving cell-to-electrode contacts.

An alternative solution would be to use a different detection scheme. Stochastics and signal processing theory have shown that the matched filter provides the optimal detection of threshold crossings. However, because the matched filter is a convolution with the time-reverse of the waveform shape, the template should already be known beforehand. This is not the case for the MEA recordings, and as such a filter bank consisting of different possible waveform shapes should be defined to test for occurrence of action potentials. As shown in the results here, waveform shapes are fairly well distinguishable, which would make this method more suitable to filter action potentials, given the low SNR.

Data analysis requires longer protocol length

The data analysis presented here has been specifically designed to handle the various issues that came up in this particular data set, such as false detection, artefacts, variable noise and bursting neurons. These problems can be prevented by recording sufficient data under constant conditions, which was not the case in this project. Activity was often elicited by applying various manipulations. Furthermore, the noise introduced by a false threshold setting made the data analysis significantly more complex. However, the problems addressed before can only be partially solved when better experimental procedures are followed. Since the activity in the striatum is very low, much longer recording times are required to collect sufficient data for statistical analysis. If more waveforms are detected, they will be less likely categorized as noise or outliers, and clustering accuracy may be improved. Additionally, statistics on interspike interval require a sufficient number of waveforms to evaluate the firing patterns. The experimenter should keep this in mind when choosing appropriate wash-in/washout times and stimulation protocol.

Chapter 6

Conclusions

In order to investigate the effect of blocking fast spiking interneurons on striatal network activity, planar microelectrode arrays were employed to record from sagittal slices of the rat striatum. This platform was chosen for its capacity to record from multiple sites in a controlled setting, but it was not known whether it was possible to mimic *in-vivo* activity in these slices. Strongly correlated input from the cortex is required to evoke activity in the striatum, which may not be the case in acute slices. In fact, the presented results show that it is often not possible to record any activity in striatal slices. In general, pharmacological and electrical stimulation were unsuccessful in reliably eliciting long term baseline activity. Nevertheless, several experiments were carried out to further understand extracellular behaviour of the striatum in acute slices. However, errors in threshold settings and low signal-to-noise ratio, as well as low detection rate have impeded data analysis of firing rates.

6.1 Slice inactivity

The causes for the low measured activity can be technical and physiological. The highly vulnerable brain tissue is put under oxidative and mechanical stress during extraction and slicing, which can lead to cell death. Although the influence of such technical issues was reduced as much as possible, this still results in a low success rate of recorded slices. However, even when experiments were carried out as carefully as possible, no stable activity was recorded in the striatum. Activity is often only recorded on a small subset of electrodes, and individual cells fire only sporadically. Consequently, it is hard to determine whether slices are still active and whether an experiment should be continued.

In order to determine slice viability and to exclude technical causes, electrical and pharmacological stimulation were applied to silent slices. When this did not succeed in eliciting activity, the striatal slice was deemed inactive. This led to very low success rates, where only 1 or 2 slices per animal were active over extended time frames. This would mean that experiments on acute slices would not be able to produce statistically significant results. However, additional experiments in the hippocampus showed that silent slices of the striatum were not dead. Despite the fact that tissue quality in the hippocampus was much lower than in the striatum, experiments on this brain area showed significantly higher success rates of spontaneous activity. Furthermore, the effects of glutamine in the hippocampus were strong and showed that diffusion in the slice is sufficient to influence activity.

Because spontaneous activity was very low in the striatum, slices were stimulated (mechanically, electrically and pharmacologically) to evoke activity. Since this had variable effects for each slice, comparisons between slices and preparation types are often invalid. Analysis of frequencies and firing patterns has not revealed any differences between lesioned and healthy slices. However, no conclusions can be drawn regarding this perceived similarity, because signals were not spontaneous and stimulation protocols were not consistent over a sufficient number of slices.

6.2 Acute slices

Although acute slices are often used to study neuronal activity, these experiments are usually performed in the hippocampus, cerebellum and cortex, which are inherently active brain structures with clear structure and function. Recordings in other structures are often done using intracellular techniques and have not been able to show network activity representative of *in-vivo* conditions. The work presented here is one of few extracellular experiments on the striatum, and has shown that this structure is a far less suitable target for network analysis in acute slices. Several aspects of the specific nature of the striatum have been under-appreciated during the literature study, but results obtained here are in line with previous reports that acute slices of the striatum do not fire spontaneously. However, this project has served to illustrate how acute slices can be better employed for neurophysiological investigations.

Overall, the presented results and literature study have shown several very fundamental issues regarding experiments on acute slices, especially in the striatum. Network activity in acute slices is more severely interrupted than previously thought, and the potential of MEA technology may not be used to its full extent. Although multiple neurons can be measured simultaneously, their spontaneous activity in acute slices does not reflect *in-vivo* downstate/upstate cycling. Rather, external stimulation is required to evoke activity in the striatum, but this will severely influence network behaviour and may obscure the very phenomena that are under investigation, such as the effect of FSI's on striatal oscillations. Application of IEM-1460 is only effective when glutamatergic input is upheld, therefore careful simulation of cortical (and thalamic) input is required to evaluate oscillations and synchrony of the striatum in healthy and parkinsonian conditions.

Measurements in acute slices suffer from poor reproducibility, because slight errors in protocol execution can be detrimental to slice quality. The fragility of the tissue and technical issues may both result in unrepresentative results, and it is important to distinguish between these sources of error. Quality assays should be applied to quantify cell survival rates.

Interestingly, both of the issues mentioned here may be alleviated by incubating slices following preparation. Previously reported studies have shown that network activity, more specifically the down/upstate cycling seen in striatal MSN's, may be restored after one day of incubation. Additionally, live-dead assays applied to incubated slices has been successfully used to determine cell survival. Although it is unsure whether incubation in growth medium reduces the effect of 6-OHDA lesions, investigations on acute slices would benefit from it. A more practical advantage of incubation is that recordings are not limited by time constraints following tissue preparation. Experiments can take more time and each slice may be evaluated more thoroughly without being compromised by tissue degradation.

Regardless of whether slice quality can be improved, it remains necessary to determine slice survival instantaneously upon transferral to the recording chamber. Several practical methods, such as testing electrical propagation may ensure slice-to-chip contact. However, stimulation of the tissue, either electrical or pharmacological, is required to determine the number of viable connections. The stimulations used in this project were unreliable, and more effective depolarizing agents might be employed to identify usable channels.

Although GABAergic interneurons in the striatum are receiving more attention as potential agents in beta oscillations, investigations on network effects have been largely limited to computational modeling. *In-vivo* blocking of FSI's has led to dystonic behaviour and evidence for the role of FSI's in Parkinson's disease is increasing. However, to fully understand the role of FSI's on network activity and in PD, an ideal measurement platform should allow a stable environment but still behave realistically. Although acute slices combined with microelectrode arrays might provide such a platform, the work presented here has shown that due to inherently low spontaneous activity, additional requirements are necessary to simulate the *in-vivo* striatum. Simulation of cortical input is essential to overcome the inherent inhibition produced by the GABAergic network. Acute slices and MEA technology might provide a well-controllable electrophysiological measurement platform, but investigations in the striatum and specifically the role of fast spiking require a slightly different approach to conventional slicing procedures.

References

- [1] Parkinson's disease foundation. Statistics on Parkinson's Disease. [Online]. Available: http://www.pdf.org/en/parkinson_statistics
- [2] C. Hammond, H. Bergman, and P. Brown, "Pathological synchronization in Parkinson's disease: networks, models and treatments," *Trends in Neurosciences*, vol. 30, no. 7, pp. 357–364, 2007. [Online]. Available: <http://www.sciencedirect.com/science/article/pii/S0166223607001233>
- [3] A. J. Lees, "Unresolved issues relating to the shaking palsy on the celebration of James Parkinson's 250th birthday." *Movement disorders : official journal of the Movement Disorder Society*, vol. 22 Suppl 1, pp. S327–34, Sep. 2007. [Online]. Available: <http://www.ncbi.nlm.nih.gov/pubmed/18175393>
- [4] H. Ehringer and O. Hornykiewicz, "Verteilung Von Noradrenalin Und Dopamin (3-Hydroxytyramin) Im Gehirn Des Menschen Und Ihr Verhalten Bei Erkrankungen Des Extrapyramidalen Systems," *Klinische Wochenschrift*, vol. 38, no. 24, pp. 1236–1239, Dec. 1960. [Online]. Available: <http://link.springer.com/10.1007/BF01485901>
- [5] M. G. Spillantini, M. L. Schmidt, V. M.-Y. Lee, J. Q. Trojanowski, R. Jakes, and M. Goedert, "[alpha]-Synuclein in Lewy bodies," vol. 388, no. 6645, pp. 839–840, Aug. 1997.
- [6] S. Shimohama, H. Sawada, Y. Kitamura, and T. Taniguchi, "Disease model: Parkinson's disease," *Trends in Molecular Medicine*, vol. 9, no. 8, pp. 360–365, Aug. 2003. [Online]. Available: <http://www.sciencedirect.com/science/article/pii/S1471491403001175>
- [7] R. Betarbet, T. B. Sherer, and J. T. Greenamyre, "Animal models of Parkinson's disease." *BioEssays : news and reviews in molecular, cellular and developmental biology*, vol. 24, no. 4, pp. 308–18, Apr. 2002. [Online]. Available: <http://www.ncbi.nlm.nih.gov/pubmed/11948617>
- [8] J. E. Ahlskog and M. D. Muentert, "Frequency of levodopa-related dyskinesias and motor fluctuations as estimated from the cumulative literature," *Movement Disorders*, vol. 16, no. 3, pp. 448–458, May 2001. [Online]. Available: <http://doi.wiley.com/10.1002/mds.1090>
- [9] N. Kumar, J. A. Van Gerpen, J. H. Bower, and J. E. Ahlskog, "Levodopa-dyskinesia incidence by age of Parkinson's disease onset." *Movement disorders : official journal of the Movement Disorder Society*, vol. 20, no. 3, pp. 342–4, Mar. 2005. [Online]. Available: <http://www.ncbi.nlm.nih.gov/pubmed/15580606>
- [10] G. Fabbrini, J. M. Brotchie, F. Grandas, M. Nomoto, and C. G. Goetz, "Levodopa-induced dyskinesias." *Movement disorders : official journal of the Movement Disorder Society*, vol. 22, no. 10, pp. 1379–89; quiz 1523, Jul. 2007. [Online]. Available: <http://www.ncbi.nlm.nih.gov/pubmed/17427940>
- [11] J. W. Mink, "The basal ganglia: focused selection and inhibition of competing motor programs," *Progress in Neurobiology*, vol. 50, no. 4, pp. 381–425, Nov. 1996. [Online]. Available: <http://www.sciencedirect.com/science/article/pii/S0301008296000421>
- [12] J. P. Bolam, J. J. Hanley, P. A. C. Booth, and M. D. Bevan, "Synaptic organisation of the basal ganglia," *Journal of Anatomy*, vol. 196, no. 4, pp. 527–542, May 2000. [Online]. Available: <http://doi.wiley.com/10.1046/j.1469-7580.2000.19640527.x>
- [13] R. L. Albin, A. B. Young, and J. B. Penney, "The functional anatomy of basal ganglia disorders," *Trends in Neurosciences*, vol. 12, no. 10, pp. 366–375, Jan. 1989. [Online]. Available: <http://www.sciencedirect.com/science/article/pii/01662236890074X>
- [14] M. R. DeLong, "Primate models of movement disorders of basal ganglia origin," *Trends in Neurosciences*, vol. 13, no. 7, pp. 281–285, Jul. 1990. [Online]. Available: <http://www.sciencedirect.com/science/article/pii/016622369090110V>
- [15] W. D. Hutchison, J. O. Dostrovsky, J. R. Walters, R. Courtemanche, T. Boraud, J. Goldberg, and P. Brown, "Neuronal oscillations in the basal ganglia and movement disorders: evidence from whole animal and human recordings." *The Journal of neuroscience : the official journal of the Society for Neuroscience*, vol. 24, no. 42, pp. 9240–3, Oct. 2004. [Online]. Available: <http://www.jneurosci.org/content/24/42/9240.full>
- [16] M. Bevan, "Move to the rhythm: oscillations in the subthalamic nucleus-external globus pallidus network," *Trends in Neurosciences*, vol. 25, no. 10, pp. 525–531, Oct. 2002. [Online]. Available: <http://www.sciencedirect.com/science/article/pii/S016622360202235X>
- [17] W. D. Hutchison, A. E. Lang, J. O. Dostrovsky, and A. M. Lozano, "Pallidal neuronal activity: implications for models of dystonia." *Annals of neurology*, vol. 53, no. 4, pp. 480–8, Apr. 2003. [Online]. Available: <http://www.ncbi.nlm.nih.gov/pubmed/12666115>
- [18] K. P. Bhatia and C. Marsden, "The behavioural and motor consequences of focal lesions of the basal ganglia in man," *Brain*, vol. 117, no. 4, pp. 859–876, Aug. 1994. [Online]. Available: <http://brain.oxfordjournals.org/content/117/4/859.short>
- [19] M. S. Baron, J. L. Vitek, R. A. Bakay, J. Green, Y. Kaneoke, T. Hashimoto, R. S. Turner, J. L. Woodard, S. A. Cole, W. M. McDonald, and M. R. DeLong, "Treatment of advanced Parkinson's disease by posterior GPi pallidotomy: 1-year results of a pilot study." *Annals of neurology*, vol. 40, no. 3, pp. 355–66, Sep. 1996. [Online]. Available: <http://www.ncbi.nlm.nih.gov/pubmed/8797525>

- [20] M. A. Belluscio, M. V. Escande, E. Keifman, L. A. Riquelme, M. G. Murer, and C. L. Zold, "Oscillations in the basal ganglia in Parkinson's disease: Role of the striatum," *Basal Ganglia*, 2013. [Online]. Available: <http://www.sciencedirect.com/science/article/pii/S221053361300138X>
- [21] H. Bergman, A. Feingold, A. Nini, A. Raz, H. Slovin, M. Abeles, and E. Vaadia, "Physiological aspects of information processing in the basal ganglia of normal and parkinsonian primates," *Trends in Neurosciences*, vol. 21, no. 1, pp. 32–38, Jan. 1998. [Online]. Available: <http://www.sciencedirect.com/science/article/pii/S016622369701151X>
- [22] R. Levy and W. Hutchison, "Synchronized neuronal discharge in the basal ganglia of parkinsonian patients is limited to oscillatory activity," *The Journal of . . .*, 2002. [Online]. Available: <http://www.jneurosci.org/content/22/7/2855.short>
- [23] T. Wichmann and J. Soares, "Neuronal firing before and after burst discharges in the monkey basal ganglia is predictably patterned in the normal state and altered in parkinsonism." *Journal of neurophysiology*, vol. 95, no. 4, pp. 2120–33, Apr. 2006. [Online]. Available: <http://jn.physiology.org/content/95/4/2120.short>
- [24] M. Fillion and L. Tremblay, "Abnormal spontaneous activity of globus pallidus neurons in monkeys with MPTP-induced parkinsonism," *Brain Research*, vol. 547, no. 1, pp. 140–144, Apr. 1991. [Online]. Available: <http://www.sciencedirect.com/science/article/pii/000689939190585J>
- [25] J. Marsden, P. Limousin-Dowsey, and P. Ashby, "Subthalamic nucleus, sensorimotor cortex and muscle interrelationships in Parkinson's disease," *Brain*, 2001. [Online]. Available: <http://brain.oxfordjournals.org/content/124/2/378.short>
- [26] D. Williams, M. Tijssen, and G. V. Bruggen, "Dopamine dependent changes in the functional connectivity between basal ganglia and cerebral cortex in humans," *Brain*, 2002. [Online]. Available: <http://brain.oxfordjournals.org/content/125/7/1558.short>
- [27] A. Schnitzler and J. Gross, "Normal and pathological oscillatory communication in the brain." *Nature reviews. Neuroscience*, vol. 6, no. 4, pp. 285–96, Apr. 2005. [Online]. Available: <http://dx.doi.org/10.1038/nrn1650>
- [28] P. Brown, "Abnormal oscillatory synchronisation in the motor system leads to impaired movement." *Current opinion in neurobiology*, vol. 17, no. 6, pp. 656–64, Dec. 2007. [Online]. Available: <http://www.sciencedirect.com/science/article/pii/S0959438807001365>
- [29] L. M. F. Doyle, A. A. Kühn, M. Hariz, A. Kupsch, G.-H. Schneider, and P. Brown, "Levodopa-induced modulation of subthalamic beta oscillations during self-paced movements in patients with Parkinson's disease." *The European journal of neuroscience*, vol. 21, no. 5, pp. 1403–12, Mar. 2005. [Online]. Available: <http://www.ncbi.nlm.nih.gov/pubmed/15813950>
- [30] A. A. Kühn, A. Kupsch, G.-H. Schneider, and P. Brown, "Reduction in subthalamic 8-35 Hz oscillatory activity correlates with clinical improvement in Parkinson's disease." *The European journal of neuroscience*, vol. 23, no. 7, pp. 1956–60, Apr. 2006. [Online]. Available: <http://www.ncbi.nlm.nih.gov/pubmed/16623853>
- [31] R. Levy, "Dependence of subthalamic nucleus oscillations on movement and dopamine in Parkinson's disease," *Brain*, vol. 125, no. 6, pp. 1196–1209, Jun. 2002. [Online]. Available: <http://brain.oxfordjournals.org/content/125/6/1196.short>
- [32] P. Brown, A. Oliviero, P. Mazzone, A. Insola, P. Tonali, and V. Di Lazzaro, "Dopamine Dependency of Oscillations between Subthalamic Nucleus and Pallidum in Parkinson's Disease," *J. Neurosci.*, vol. 21, no. 3, pp. 1033–1038, Feb. 2001. [Online]. Available: <http://www.jneurosci.org/content/21/3/1033.short>
- [33] A. A. Kühn, F. Kempf, C. Brücke, L. Gaynor Doyle, I. Martinez-Torres, A. Pogosyan, T. Trottenberg, A. Kupsch, G.-H. Schneider, M. I. Hariz, W. Vandenberghe, B. Nuttin, and P. Brown, "High-frequency stimulation of the subthalamic nucleus suppresses oscillatory beta activity in patients with Parkinson's disease in parallel with improvement in motor performance." *The Journal of neuroscience : the official journal of the Society for Neuroscience*, vol. 28, no. 24, pp. 6165–73, Jun. 2008. [Online]. Available: <http://www.jneurosci.org/content/28/24/6165.short>
- [34] C. C. Chen, V. Litvak, T. Gilbertson, A. Kühn, C. S. Lu, S. T. Lee, C. H. Tsai, S. Tisch, P. Limousin, M. Hariz, and P. Brown, "Excessive synchronization of basal ganglia neurons at 20 Hz slows movement in Parkinson's disease." *Experimental neurology*, vol. 205, no. 1, pp. 214–21, May 2007. [Online]. Available: <http://www.sciencedirect.com/science/article/pii/S0014488607000581>
- [35] A. Pogosyan, L. D. Gaynor, A. Eusebio, and P. Brown, "Boosting cortical activity at Beta-band frequencies slows movement in humans." *Current biology : CB*, vol. 19, no. 19, pp. 1637–41, Oct. 2009. [Online]. Available: <http://www.sciencedirect.com/science/article/pii/S0960982209016996>
- [36] S. Baker, E. Olivier, and R. Lemon, "Coherent oscillations in monkey motor cortex and hand muscle EMG show task-dependent modulation." *The Journal of Physiology*, 1997. [Online]. Available: http://jp.physoc.org/content/501/Pt_1/225.short
- [37] N. Swann and N. Tandon, "Intracranial EEG reveals a time- and frequency-specific role for the right inferior frontal gyrus and primary motor cortex in stopping initiated responses," *The Journal of . . .*, 2009. [Online]. Available: <http://www.jneurosci.org/content/29/40/12675.short>
- [38] D. K. Leventhal, G. J. Gage, R. Schmidt, J. R. Pettibone, A. C. Case, and J. D. Berke, "Basal ganglia beta oscillations accompany cue utilization." *Neuron*, vol. 73, no. 3, pp. 523–36, Feb. 2012. [Online]. Available: <http://www.sciencedirect.com/science/article/pii/S0896627312000360>
- [39] M. Rivlin-Etzion, O. Marmor, G. Heimer, A. Raz, A. Nini, and H. Bergman, "Basal ganglia oscillations and pathophysiology of movement disorders." *Current opinion in neurobiology*, vol. 16, no. 6, pp. 629–37, Dec. 2006. [Online]. Available: <http://www.sciencedirect.com/science/article/pii/S0959438806001401>
- [40] R. C. Helmich, M. Hallett, G. Deuschl, I. Toni, and B. R. Bloem, "Cerebral causes and consequences of parkinsonian resting tremor: a tale of two circuits?" *Brain : a journal of neurology*, vol. 135, no. Pt 11, pp. 3206–26, Nov. 2012. [Online]. Available: <http://brain.oxfordjournals.org/content/135/11/3206.short>
- [41] T. Wu and M. Hallett, "The cerebellum in Parkinson's disease." *Brain : a journal of neurology*, vol. 136, no. Pt 3, pp. 696–709, Mar. 2013. [Online]. Available: <http://brain.oxfordjournals.org/content/136/3/696.short>

- [42] W. D. Hutchison, R. J. Allan, H. Opitz, R. Levy, J. O. Dostrovsky, A. E. Lang, and A. M. Lozano, "Neurophysiological identification of the subthalamic nucleus in surgery for Parkinson's disease." *Annals of neurology*, vol. 44, no. 4, pp. 622–8, Oct. 1998. [Online]. Available: <http://www.ncbi.nlm.nih.gov/pubmed/9778260>
- [43] H. Bergman, T. Wichmann, and M. DeLong, "Reversal of experimental parkinsonism by lesions of the subthalamic nucleus," *Science*, 1990. [Online]. Available: http://www.researchgate.net/publication/20752745_Reversal_of_experimental_parkinsonism_by_lesions_of_the_subthalamic_nucleus/file/9c96052584ecdb294e.pdf
- [44] N. Lemaire, L. F. Hernandez, D. Hu, Y. Kubota, M. W. Howe, and A. M. Graybiel, "Effects of dopamine depletion on LFP oscillations in striatum are task- and learning-dependent and selectively reversed by L-DOPA." *Proceedings of the National Academy of Sciences of the United States of America*, vol. 109, no. 44, pp. 18 126–31, Oct. 2012. [Online]. Available: <http://www.pnas.org/content/109/44/18126.short>
- [45] R. M. Costa, S.-C. Lin, T. D. Sotnikova, M. Cyr, R. R. Gainetdinov, M. G. Caron, and M. A. L. Nicolelis, "Rapid alterations in corticostriatal ensemble coordination during acute dopamine-dependent motor dysfunction." *Neuron*, vol. 52, no. 2, pp. 359–69, Oct. 2006. [Online]. Available: <http://www.sciencedirect.com/science/article/pii/S0896627306006295>
- [46] J. M. Burkhardt, C. Constantinidis, K. K. Anstrom, D. C. S. Roberts, and D. J. Woodward, "Synchronous oscillations and phase reorganization in the basal ganglia during akinesia induced by high-dose haloperidol." *The European journal of neuroscience*, vol. 26, no. 7, pp. 1912–24, Oct. 2007. [Online]. Available: <http://www.ncbi.nlm.nih.gov/pubmed/17897397>
- [47] A. Nini, A. Feingold, H. Slovin, and H. Bergman, "Neurons in the globus pallidus do not show correlated activity in the normal monkey, but phase-locked oscillations appear in the MPTP model of parkinsonism," *J Neurophysiol*, vol. 74, no. 4, pp. 1800–1805, Oct. 1995. [Online]. Available: <http://jn.physiology.org/content/74/4/1800>
- [48] N. Mallet, A. Pogosyan, L. F. Márton, J. P. Bolam, P. Brown, and P. J. Magill, "Parkinsonian beta oscillations in the external globus pallidus and their relationship with subthalamic nucleus activity." *The Journal of neuroscience : the official journal of the Society for Neuroscience*, vol. 28, no. 52, pp. 14 245–58, Dec. 2008. [Online]. Available: <http://www.jneurosci.org/content/28/52/14245.short>
- [49] A. J. N. Holgado, J. R. Terry, and R. Bogacz, "Conditions for the generation of beta oscillations in the subthalamic nucleus-globus pallidus network." *The Journal of neuroscience : the official journal of the Society for Neuroscience*, vol. 30, no. 37, pp. 12 340–52, Sep. 2010. [Online]. Available: <http://www.jneurosci.org/content/30/37/12340.short>
- [50] D. Terman, J. E. Rubin, A. C. Yew, and C. J. Wilson, "Activity Patterns in a Model for the Subthalamopallidal Network of the Basal Ganglia," *J. Neurosci.*, vol. 22, no. 7, pp. 2963–2976, Apr. 2002. [Online]. Available: <http://www.jneurosci.org/content/22/7/2963.short>
- [51] M. D. Humphries, R. D. Stewart, and K. N. Gurney, "A physiologically plausible model of action selection and oscillatory activity in the basal ganglia." *The Journal of neuroscience : the official journal of the Society for Neuroscience*, vol. 26, no. 50, pp. 12 921–42, Dec. 2006. [Online]. Available: <http://www.jneurosci.org/content/26/50/12921.short>
- [52] J. Soares, M. A. Kliem, R. Betarbet, J. T. Greenamyre, B. Yamamoto, and T. Wichmann, "Role of external pallidal segment in primate parkinsonism: comparison of the effects of 1-methyl-4-phenyl-1,2,3,6-tetrahydropyridine-induced parkinsonism and lesions of the external pallidal segment." *The Journal of neuroscience : the official journal of the Society for Neuroscience*, vol. 24, no. 29, pp. 6417–26, Jul. 2004. [Online]. Available: <http://www.jneurosci.org/content/24/29/6417.short>
- [53] P. Magill, J. Bolam, and M. Bevan, "Dopamine regulates the impact of the cerebral cortex on the subthalamic nucleus-globus pallidus network," *Neuroscience*, vol. 106, no. 2, pp. 313–330, Sep. 2001. [Online]. Available: <http://www.sciencedirect.com/science/article/pii/S0306452201002810>
- [54] K. Y. Tseng, F. Kasanetz, L. Kargieman, L. A. Riquelme, and M. G. Murer, "Cortical slow oscillatory activity is reflected in the membrane potential and spike trains of striatal neurons in rats with chronic nigrostriatal lesions," *Journal of Neuroscience*, vol. 21, no. 16, pp. 6430–6439, 2001. [Online]. Available: <http://www.scopus.com/inward/record.url?eid=2-s2.0-0035882528&partnerID=tZOTx3y1>
- [55] J. M. Tepper and J. P. Bolam, "Functional diversity and specificity of neostriatal interneurons." *Current opinion in neurobiology*, vol. 14, no. 6, pp. 685–92, Dec. 2004. [Online]. Available: <http://www.sciencedirect.com/science/article/pii/S0959438804001552>
- [56] C. R. Gerfen, "Synaptic organization of the striatum." *Journal of electron microscopy technique*, vol. 10, no. 3, pp. 265–81, Nov. 1988. [Online]. Available: <http://www.ncbi.nlm.nih.gov/pubmed/3069970>
- [57] V. V. Rymer, R. Sasseville, K. C. Luk, and A. F. Sadikot, "Neurogenesis and stereological morphometry of calretinin-immunoreactive GABAergic interneurons of the neostriatum." *The Journal of comparative neurology*, vol. 469, no. 3, pp. 325–39, Feb. 2004. [Online]. Available: <http://www.ncbi.nlm.nih.gov/pubmed/14730585>
- [58] R. Preston, G. Bishop, and S. Kitai, "Medium spiny neuron projection from the rat striatum: An intracellular horseradish peroxidase study," *Brain Research*, vol. 183, no. 2, pp. 253–263, Feb. 1980. [Online]. Available: <http://www.sciencedirect.com/science/article/pii/000689938090462X>
- [59] H. Steiner and C. R. Gerfen, "Role of dynorphin and enkephalin in the regulation of striatal output pathways and behavior," *Experimental Brain Research*, vol. 123, no. 1-2, pp. 60–76, Oct. 1998. [Online]. Available: <http://link.springer.com/10.1007/s002210050545>
- [60] C. Gerfen, J. McGinty, and d. Young, WS, "Dopamine differentially regulates dynorphin, substance P, and enkephalin expression in striatal neurons: in situ hybridization histochemical analysis," *J. Neurosci.*, vol. 11, no. 4, pp. 1016–1031, Apr. 1991. [Online]. Available: <http://www.jneurosci.org/content/11/4/1016.short>
- [61] Y. Kawaguchi, "Neostriatal cell subtypes and their functional roles," *Neuroscience Research*, vol. 27, no. 1, pp. 1–8, Jan. 1997. [Online]. Available: <http://www.sciencedirect.com/science/article/pii/S0168010296011340>

- [62] J. D. Berke, M. Okatan, J. Skurski, and H. B. Eichenbaum, "Oscillatory entrainment of striatal neurons in freely moving rats." *Neuron*, vol. 43, no. 6, pp. 883–96, Sep. 2004. [Online]. Available: <http://www.sciencedirect.com/science/article/pii/S0896627304005628>
- [63] A. B. Wiltschko, J. R. Pettibone, and J. D. Berke, "Opposite effects of stimulant and antipsychotic drugs on striatal fast-spiking interneurons." *Neuropsychopharmacology : official publication of the American College of Neuropsychopharmacology*, vol. 35, no. 6, pp. 1261–70, May 2010. [Online]. Available: <http://dx.doi.org/10.1038/npp.2009.226>
- [64] O. Yarom and D. Cohen, "Putative cholinergic interneurons in the ventral and dorsal regions of the striatum have distinct roles in a two choice alternative association task." *Frontiers in systems neuroscience*, vol. 5, p. 36, Jan. 2011. [Online]. Available: <http://journal.frontiersin.org/Journal/10.3389/fnsys.2011.00036/abstract>
- [65] L. A. Tellez, I. O. Perez, S. A. Simon, and R. Gutierrez, "Transitions between sleep and feeding states in rat ventral striatum neurons." *Journal of neurophysiology*, vol. 108, no. 6, pp. 1739–51, Sep. 2012. [Online]. Available: <http://jn.physiology.org/content/108/6/1739.figures-only>
- [66] D. F. English, O. Ibanez-Sandoval, E. Stark, F. Tecuapetla, G. Buzsáki, K. Deisseroth, J. M. Tepper, and T. Koos, "GABAergic circuits mediate the reinforcement-related signals of striatal cholinergic interneurons." *Nature neuroscience*, vol. 15, no. 1, pp. 123–30, Jan. 2012. [Online]. Available: <http://dx.doi.org/10.1038/nn.2984>
- [67] D. Yael, D. H. Zeef, D. Sand, A. Moran, D. B. Katz, D. Cohen, Y. Temel, and I. Bar-Gad, "Haloperidol-induced changes in neuronal activity in the striatum of the freely moving rat." *Frontiers in systems neuroscience*, vol. 7, p. 110, Jan. 2013. [Online]. Available: <http://journal.frontiersin.org/Journal/10.3389/fnsys.2013.00110/abstract>
- [68] G. Morris, D. Arkadir, A. Nevet, E. Vaadia, and H. Bergman, "Coincident but distinct messages of midbrain dopamine and striatal tonically active neurons." *Neuron*, vol. 43, no. 1, pp. 133–43, Jul. 2004. [Online]. Available: <http://www.ncbi.nlm.nih.gov/pubmed/15233923>
- [69] J. A. Goldberg and J. N. J. Reynolds, "Spontaneous firing and evoked pauses in the tonically active cholinergic interneurons of the striatum." *Neuroscience*, vol. 198, pp. 27–43, Dec. 2011. [Online]. Available: <http://www.ncbi.nlm.nih.gov/pubmed/21925242>
- [70] B. Bennett, "Intrinsic membrane properties underlying spontaneous tonic firing in neostriatal cholinergic interneurons," *The Journal of ...*, 2000. [Online]. Available: <http://www.jneurosci.org/content/20/22/8493.short>
- [71] C. Wilson, "The mechanism of intrinsic amplification of hyperpolarizations and spontaneous bursting in striatal cholinergic interneurons," *Neuron*, 2005. [Online]. Available: <http://www.sciencedirect.com/science/article/pii/S0896627305000668>
- [72] T. Koos and J. M. Tepper, "Dual Cholinergic Control of Fast-Spiking Interneurons in the Neostriatum," *J. Neurosci.*, vol. 22, no. 2, pp. 529–535, Jan. 2002. [Online]. Available: <http://www.jneurosci.org/content/22/2/529.short>
- [73] K. Luk and A. Sadikot, "GABA promotes survival but not proliferation of parvalbumin-immunoreactive interneurons in rodent neostriatum: an in vivo study with stereology," *Neuroscience*, vol. 104, no. 1, pp. 93–103, Apr. 2001. [Online]. Available: <http://www.sciencedirect.com/science/article/pii/S0306452201000380>
- [74] G. J. Gage, C. R. Stoetznner, A. B. Wiltschko, and J. D. Berke, "Selective activation of striatal fast-spiking interneurons during choice execution." *Neuron*, vol. 67, no. 3, pp. 466–79, Aug. 2010. [Online]. Available: <http://www.sciencedirect.com/science/article/pii/S0896627310005180>
- [75] A. H. Gittis, A. B. Nelson, M. T. Thwin, J. J. Palop, and A. C. Kreitzer, "Distinct roles of GABAergic interneurons in the regulation of striatal output pathways." *The Journal of neuroscience : the official journal of the Society for Neuroscience*, vol. 30, no. 6, pp. 2223–34, Feb. 2010. [Online]. Available: <http://www.pubmedcentral.nih.gov/articlerender.fcgi?artid=2836801&tool=pmcentrez&rendertype=abstract>
- [76] T. Koós and J. M. Tepper, "Inhibitory control of neostriatal projection neurons by GABAergic interneurons." *Nature neuroscience*, vol. 2, no. 5, pp. 467–72, May 1999. [Online]. Available: <http://dx.doi.org/10.1038/8138>
- [77] A. H. Gittis, D. K. Leventhal, B. A. Fensterheim, J. R. Pettibone, J. D. Berke, and A. C. Kreitzer, "Selective inhibition of striatal fast-spiking interneurons causes dyskinesias." *The Journal of neuroscience : the official journal of the Society for Neuroscience*, vol. 31, no. 44, pp. 15727–31, Nov. 2011. [Online]. Available: <http://www.jneurosci.org/content/31/44/15727.short>
- [78] H. Planert, S. N. Szydlowski, J. J. J. Hjorth, S. Grillner, and G. Silberberg, "Dynamics of synaptic transmission between fast-spiking interneurons and striatal projection neurons of the direct and indirect pathways." *The Journal of neuroscience : the official journal of the Society for Neuroscience*, vol. 30, no. 9, pp. 3499–507, Mar. 2010. [Online]. Available: <http://www.jneurosci.org/content/30/9/3499.full>
- [79] B. Bennett and J. Bolam, "Synaptic input and output of parvalbumin-immunoreactive neurons in the neostriatum of the rat," *Neuroscience*, vol. 62, no. 3, pp. 707–719, Oct. 1994. [Online]. Available: <http://www.sciencedirect.com/science/article/pii/S0306452294904715>
- [80] S. N. Szydlowski, I. Pollak Dorocic, H. Planert, M. Carlén, K. Meletis, and G. Silberberg, "Target selectivity of feedforward inhibition by striatal fast-spiking interneurons." *The Journal of neuroscience : the official journal of the Society for Neuroscience*, vol. 33, no. 4, pp. 1678–83, Jan. 2013. [Online]. Available: <http://www.jneurosci.org/content/33/4/1678.short>
- [81] Y. Kawaguchi, C. J. Wilson, S. J. Augood, and P. C. Emson, "Striatal interneurons: chemical, physiological and morphological characterization," *Trends in Neurosciences*, vol. 18, no. 12, pp. 527–535, Dec. 1995. [Online]. Available: <http://www.sciencedirect.com/science/article/pii/0166223695983748>
- [82] C. L. Zold, M. V. Escande, P. E. Pomata, L. A. Riquelme, and M. G. Murer, "Striatal NMDA receptors gate cortico-pallidal synchronization in a rat model of Parkinson's disease," *Neurobiology of Disease*, vol. 47, no. 1, pp. 38–48, 2012. [Online]. Available: <http://www.sciencedirect.com/science/article/pii/S0969996112000939>

- [83] A. Sharott, C. K. E. Moll, G. Engler, M. Denker, S. Grün, and A. K. Engel, "Different subtypes of striatal neurons are selectively modulated by cortical oscillations." *The Journal of neuroscience : the official journal of the Society for Neuroscience*, vol. 29, no. 14, pp. 4571–85, Apr. 2009. [Online]. Available: <http://www.jneurosci.org/content/29/14/4571.short>
- [84] C. L. Zold, B. Ballion, L. A. Riquelme, F. Gonon, and M. G. Murer, "Nigrostriatal lesion induces D2-modulated phase-locked activity in the basal ganglia of rats." *The European journal of neuroscience*, vol. 25, no. 7, pp. 2131–44, Apr. 2007. [Online]. Available: <http://www.ncbi.nlm.nih.gov/pubmed/17439497>
- [85] J. Walters, D. Hu, C. Itoga, L. Parr-Brownlie, and D. Bergstrom, "Phase relationships support a role for coordinated activity in the indirect pathway in organizing slow oscillations in basal ganglia output after loss of dopamine," *Neuroscience*, vol. 144, no. 2, pp. 762–776, 2007. [Online]. Available: <http://www.sciencedirect.com/science/article/pii/S0306452206013601>
- [86] R. Courtemanche, N. Fujii, and A. M. Graybiel, "Synchronous, Focally Modulated {beta}-Band Oscillations Characterize Local Field Potential Activity in the Striatum of Awake Behaving Monkeys," *J. Neurosci.*, vol. 23, no. 37, pp. 11 741–11 752, Dec. 2003. [Online]. Available: <http://www.jneurosci.org/content/23/37/11741.short>
- [87] X.-J. Wang and J. Rinzel, "Alternating and Synchronous Rhythms in Reciprocally Inhibitory Model Neurons," *Neural Computation*, vol. 4, no. 1, pp. 84–97, Jan. 1992. [Online]. Available: <http://www.mitpressjournals.org/doi/abs/10.1162/neco.1992.4.1.84#.VIGVcDGG-So>
- [88] D. D. Pervouchine, T. I. Netoff, H. G. Rotstein, J. A. White, M. O. Cunningham, M. A. Whittington, and N. J. Kopell, "Low-dimensional maps encoding dynamics in entorhinal cortex and hippocampus." *Neural computation*, vol. 18, no. 11, pp. 2617–50, Nov. 2006. [Online]. Available: <http://www.mitpressjournals.org/doi/abs/10.1162/neco.2006.18.11.2617>
- [89] M. M. McCarthy, E. N. Brown, and N. Kopell, "Potential network mechanisms mediating electroencephalographic beta rhythm changes during propofol-induced paradoxical excitation." *The Journal of neuroscience : the official journal of the Society for Neuroscience*, vol. 28, no. 50, pp. 13 488–504, Dec. 2008. [Online]. Available: <http://www.jneurosci.org/content/28/50/13488.short>
- [90] M. M. McCarthy, C. Moore-Kochlacs, X. Gu, E. S. Boyden, X. Han, and N. Kopell, "Striatal origin of the pathologic beta oscillations in Parkinson's disease." *Proceedings of the National Academy of Sciences of the United States of America*, vol. 108, no. 28, pp. 11 620–5, Jul. 2011. [Online]. Available: <http://www.pnas.org/content/108/28/11620.short>
- [91] E. Fino, J. Glowinski, and L. Venance, "Effects of acute dopamine depletion on the electrophysiological properties of striatal neurons." *Neuroscience research*, vol. 58, no. 3, pp. 305–16, Jul. 2007. [Online]. Available: <http://www.sciencedirect.com/science/article/pii/S0168010207001265>
- [92] S. Damodaran, R. C. Evans, and K. T. Blackwell, "Synchronized firing of fast-spiking interneurons is critical to maintain balanced firing between direct and indirect pathway neurons of the striatum." *Journal of neurophysiology*, vol. 111, no. 4, pp. 836–48, Feb. 2014. [Online]. Available: <http://jn.physiology.org/content/111/4/836.abstract>
- [93] M. D. Humphries, R. Wood, and K. Gurney, "Dopamine-modulated dynamic cell assemblies generated by the GABAergic striatal microcircuit." *Neural networks : the official journal of the International Neural Network Society*, vol. 22, no. 8, pp. 1174–88, Oct. 2009. [Online]. Available: <http://www.sciencedirect.com/science/article/pii/S0893608009001646>
- [94] M. A. Nicolelis, A. A. Ghazanfar, B. M. Faggin, S. Votaw, and L. M. Oliveira, "Reconstructing the Engram: Simultaneous, Multisite, Many Single Neuron Recordings," *Neuron*, vol. 18, no. 4, pp. 529–537, Apr. 1997. [Online]. Available: <http://www.sciencedirect.com/science/article/pii/S0896627300802950>
- [95] C. Holscher, R. Anwyl, and M. J. Rowan, "Stimulation on the Positive Phase of Hippocampal Theta Rhythm Induces Long-Term Potentiation That Can Be Depotentiated by Stimulation on the Negative Phase in Area CA1 In Vivo," *J. Neurosci.*, vol. 17, no. 16, pp. 6470–6477, Aug. 1997. [Online]. Available: <http://www.jneurosci.org/content/17/16/6470.short>
- [96] C. C. McIntyre, M. Savasta, B. L. Walter, and J. L. Vitek, "How does deep brain stimulation work? Present understanding and future questions," *Journal of Clinical Neurophysiology*, vol. 21, no. 1, pp. 40–50, 2004.
- [97] T. Loddenkemper, A. Pan, S. Neme, K. B. Baker, A. R. Rezai, D. S. Dinner, E. B. Montgomery Jr, and H. O. Lüders, "Deep brain stimulation in epilepsy," *Journal of Clinical Neurophysiology*, vol. 18, no. 6, pp. 514–532, 2001.
- [98] M. A. Lebedev and M. A. L. Nicolelis, "Brain-machine interfaces: past, present and future." *Trends in neurosciences*, vol. 29, no. 9, pp. 536–46, Sep. 2006. [Online]. Available: <http://www.ncbi.nlm.nih.gov/pubmed/16859758>
- [99] D. Pleniz and S. T. Kitai, "Up and Down States in Striatal Medium Spiny Neurons Simultaneously Recorded with Spontaneous Activity in Fast-Spiking Interneurons Studied in Cortex-Striatum-Substantia Nigra Organotypic Cultures," *J. Neurosci.*, vol. 18, no. 1, pp. 266–283, Jan. 1998. [Online]. Available: <http://www.jneurosci.org/content/18/1/266.short>
- [100] C. Beurrier, Y. Ben-Ari, and C. Hammond, "Preservation of the direct and indirect pathways in an in vitro preparation of the mouse basal ganglia." *Neuroscience*, vol. 140, no. 1, pp. 77–86, Jun. 2006. [Online]. Available: <http://www.sciencedirect.com/science/article/pii/S0306452206001953>
- [101] F. O. Morin, Y. Takamura, and E. Tamiya, "Investigating neuronal activity with planar microelectrode arrays: achievements and new perspectives." *Journal of bioscience and bioengineering*, vol. 100, no. 2, pp. 131–43, Aug. 2005. [Online]. Available: <http://www.sciencedirect.com/science/article/pii/S1389172305704424>
- [102] I. L. Jones, P. Livi, M. K. Lewandowska, M. Fiscella, B. Roscic, and A. Hierlemann, "The potential of microelectrode arrays and microelectronics for biomedical research and diagnostics." *Analytical and bioanalytical chemistry*, vol. 399, no. 7, pp. 2313–29, Mar. 2011. [Online]. Available: <http://www.ncbi.nlm.nih.gov/pubmed/20676620>
- [103] M. E. J. Obien, K. Deligkaris, T. Bullmann, D. J. Bakkum, and U. Frey, "Revealing neuronal function through microelectrode array recordings," *Frontiers in Neuroscience*, vol. 8, Jan. 2015. [Online]. Available: <http://journal.frontiersin.org/Journal/10.3389/fnins.2014.00423/abstract>

- [104] U. Frey, J. Sedivy, F. Heer, R. Pedron, M. Ballini, J. Mueller, D. Bakkum, S. Hafizovic, F. D. Faraci, F. Greve, K.-U. Kirstein, and A. Hierlemann, "Switch-Matrix-Based High-Density Microelectrode Array in CMOS Technology," *IEEE Journal of Solid-State Circuits*, vol. 45, no. 2, pp. 467–482, Feb. 2010. [Online]. Available: <http://dx.doi.org/10.1109/JSSC.2009.2035196http://ieeexplore.ieee.org/lpdocs/epic03/wrapper.htm?arnumber=5405139>
- [105] M. Ballini, J. Muller, P. Livi, Y. Chen, U. Frey, A. Shadmani, I. Jones, W. Gong, M. Fiscella, M. Radivojevic, D. Bakkum, A. Stettler, F. Heer, and A. Hierlemann, "A 1024-channel CMOS microelectrode-array system with 26'400 electrodes for recording and stimulation of electro-active cells in-vitro," pp. C54–C55, 2013.
- [106] K. K. Skrede and R. H. Westgaard, "The transverse hippocampal slice: a well-defined cortical structure maintained in vitro." *Brain research*, vol. 35, no. 2, pp. 589–93, Dec. 1971. [Online]. Available: <http://www.ncbi.nlm.nih.gov/pubmed/5135556>
- [107] M. O. Heuschkel, M. Fejtli, M. Raggenbass, D. Bertrand, and P. Renaud, "A three-dimensional multi-electrode array for multi-site stimulation and recording in acute brain slices," *Journal of Neuroscience Methods*, vol. 114, no. 2, pp. 135–148, Mar. 2002. [Online]. Available: <http://www.sciencedirect.com/science/article/pii/S0165027001005143>
- [108] H. Oka, K. Shimono, R. Ogawa, H. Sugihara, and M. Taketani, "A new planar multielectrode array for extracellular recording: application to hippocampal acute slice," *Journal of Neuroscience Methods*, vol. 93, no. 1, pp. 61–67, Oct. 1999. [Online]. Available: <http://www.sciencedirect.com/science/article/pii/S0165027099001132>
- [109] E. I. Moser, "The multi-laned hippocampus." *Nature neuroscience*, vol. 14, no. 4, pp. 407–8, Apr. 2011. [Online]. Available: http://www.nature.com/neuro/journal/v14/n4/full/nn.2783.html?message-global=remove&WT.ec_id=NEURO-201104
- [110] N. Dehorter, C. Guigoni, C. Lopez, J. Hirsch, A. Eusebio, Y. Ben-Ari, and C. Hammond, "Dopamine-deprived striatal GABAergic interneurons burst and generate repetitive gigantic IPSCs in medium spiny neurons." *The Journal of neuroscience : the official journal of the Society for Neuroscience*, vol. 29, no. 24, pp. 7776–87, Jun. 2009. [Online]. Available: <http://www.jneurosci.org/content/29/24/7776.full>
- [111] R. Smith and E. Bracci, "Multi Electrode Array recordings from the striatum and adjacent anatomical areas." *Proceedings of The Physiological Society*, vol. Proc Physi, 2011. [Online]. Available: <http://www.physoc.org/2nd-life-sciences-investigations-internal-audits-forum/proceedings/abstract/ProcPhysiolSoc23PC56>
- [112] M. S. Lewicki, "A review of methods for spike sorting: the detection and classification of neural action potentials." *Network (Bristol, England)*, vol. 9, no. 4, pp. R53–78, Nov. 1998. [Online]. Available: <http://www.ncbi.nlm.nih.gov/pubmed/10221571>
- [113] M. C. Quirk, D. L. Sosulski, C. E. Feierstein, N. Uchida, and Z. F. Mainen, "A defined network of fast-spiking interneurons in orbitofrontal cortex: responses to behavioral contingencies and ketamine administration." *Frontiers in systems neuroscience*, vol. 3, p. 13, Jan. 2009. [Online]. Available: <http://www.pubmedcentral.nih.gov/articlerender.fcgi?artid=2802551&tool=pmcentrez&rendertype=abstract>
- [114] A. Tankus, Y. Yeshurun, and I. Fried, "An automatic measure for classifying clusters of suspected spikes into single cells versus multiunits." *Journal of neural engineering*, vol. 6, no. 5, p. 056001, Oct. 2009. [Online]. Available: <http://stacks.iop.org/1741-2552/6/i=5/a=056001>
- [115] R. Quiroga, "Spike sorting," *Scholarpedia*, vol. 2, no. 12, p. 3583, Dec. 2007. [Online]. Available: http://www.scholarpedia.org/article/Spike_sorting
- [116] D. N. Hill, S. B. Mehta, and D. Kleinfeld, "Quality metrics to accompany spike sorting of extracellular signals." *The Journal of neuroscience : the official journal of the Society for Neuroscience*, vol. 31, no. 24, pp. 8699–705, Jun. 2011. [Online]. Available: <http://www.pubmedcentral.nih.gov/articlerender.fcgi?artid=3123734&tool=pmcentrez&rendertype=abstract>
- [117] Y. Kaneoke and J. Vitek, "Burst and oscillation as disparate neuronal properties," *Journal of Neuroscience Methods*, vol. 68, no. 2, pp. 211–223, Oct. 1996. [Online]. Available: <http://www.sciencedirect.com/science/article/pii/S0165027096000817>
- [118] L. Chen, Y. Deng, W. Luo, Z. Wang, and S. Zeng, "Detection of bursts in neuronal spike trains by the mean inter-spike interval method," *Progress in Natural Science*, vol. 19, no. 2, pp. 229–235, Feb. 2009. [Online]. Available: <http://www.sciencedirect.com/science/article/pii/S1002007108003432>
- [119] D. J. Bakkum, M. Radivojevic, U. Frey, F. Franke, A. Hierlemann, and H. Takahashi, "Parameters for burst detection." *Frontiers in computational neuroscience*, vol. 7, p. 193, Jan. 2013. [Online]. Available: <http://www.pubmedcentral.nih.gov/articlerender.fcgi?artid=3915237&tool=pmcentrez&rendertype=abstract>
- [120] E. Schneidman, M. J. Berry, R. Segev, and W. Bialek, "Weak pairwise correlations imply strongly correlated network states in a neural population." *Nature*, vol. 440, no. 7087, pp. 1007–12, Apr. 2006. [Online]. Available: <http://dx.doi.org/10.1038/nature04701>
- [121] A. Gittis, G. Hang, E. LaDow, L. Shoenfeld, B. Atallah, S. Finkbeiner, and A. Kreitzer, "Rapid Target-Specific Remodeling of Fast-Spiking Inhibitory Circuits after Loss of Dopamine," *Neuron*, vol. 71, no. 5, pp. 858–868, 2011. [Online]. Available: <http://www.sciencedirect.com/science/article/pii/S0896627311005654>
- [122] P. Andersen, T. Bliss, and K. Skrede, "Lamellar organization of hippocampal excitatory pathways," *Experimental Brain Research*, vol. 13, no. 2, Aug. 1971. [Online]. Available: <http://link.springer.com/10.1007/BF00234087>
- [123] U. Egert, D. Heck, and A. Aertsen, "Two-dimensional monitoring of spiking networks in acute brain slices." *Experimental brain research*, vol. 142, no. 2, pp. 268–74, Jan. 2002. [Online]. Available: <http://www.ncbi.nlm.nih.gov/pubmed/11807580>
- [124] K. Fukunaga and L. Hostetler, "The estimation of the gradient of a density function, with applications in pattern recognition," *IEEE Transactions on Information Theory*, vol. 21, no. 1, pp. 32–40, Jan. 1975. [Online]. Available: <http://ieeexplore.ieee.org/articleDetails.jsp?arnumber=1055330>
- [125] A. De Simoni, C. B. Griesinger, and F. A. Edwards, "Development of rat CA1 neurones in acute versus organotypic slices: role of experience in synaptic morphology and activity." *The Journal of physiology*, vol. 550, no. Pt 1, pp. 135–47, Jul. 2003. [Online]. Available: <http://www.pubmedcentral.nih.gov/articlerender.fcgi?artid=2343027&tool=pmcentrez&rendertype=abstract>

- [126] D. M. Mathis, J. L. Furman, and C. M. Norris, "Preparation of acute hippocampal slices from rats and transgenic mice for the study of synaptic alterations during aging and amyloid pathology." *Journal of visualized experiments : JoVE*, no. 49, p. e2330, Jan. 2011. [Online]. Available: <http://www.jove.com/video/2330/preparation-acute-hippocampal-slices-from-rats-transgenic-mice-for>
- [127] A. Villers and L. Ris, "Improved preparation and preservation of hippocampal mouse slices for a very stable and reproducible recording of long-term potentiation." *Journal of visualized experiments : JoVE*, no. 76, p. e50483, Jan. 2013. [Online]. Available: <http://www.jove.com/video/50483/improved-preparation-preservation-hippocampal-mouse-slices-for-very>
- [128] Y. Xie, T. Heida, J. Stegenga, Y. Zhao, A. Moser, V. Tronnier, T. J. Feuerstein, and U. G. Hofmann, "High-frequency electrical stimulation suppresses cholinergic accumbens interneurons in acute rat brain slices through GABAB receptors." *The European journal of neuroscience*, Sep. 2014. [Online]. Available: <http://www.ncbi.nlm.nih.gov/pubmed/25251290>
- [129] C. R. Gerfen and C. J. Wilson, *Integrated systems of the CNS, part III - Cerebellum, basal ganglia, olfactory system*, ser. Handbook of Chemical Neuroanatomy. Elsevier, 1996, vol. 12. [Online]. Available: <http://www.sciencedirect.com/science/article/pii/S0924819696800042>
- [130] C. J. Wilson and P. M. Groves, "Spontaneous firing patterns of identified spiny neurons in the rat neostriatum," *Brain Research*, vol. 220, no. 1, pp. 67–80, Sep. 1981. [Online]. Available: <http://www.sciencedirect.com/science/article/pii/0006899381902110>
- [131] P. Calabresi, R. Maj, A. Pisani, N. Mercuri, and G. Bernardi, "Long-term synaptic depression in the striatum: physiological and pharmacological characterization," *J. Neurosci.*, vol. 12, no. 11, pp. 4224–4233, Nov. 1992. [Online]. Available: <http://www.jneurosci.org/content/12/11/4224.short>
- [132] F. E. Randall, M. Garcia-Munoz, C. Vickers, S. C. Schock, W. A. Staines, and G. W. Arbuthnott, "The Corticostriatal System in Dissociated Cell Culture," *Frontiers in Systems Neuroscience*, vol. 5, p. 52, Jan. 2011. [Online]. Available: <http://www.pubmedcentral.nih.gov/articlerender.fcgi?artid=3127227&tool=pmcentrez&rendertype=abstract>
- [133] C. Wilson and Y. Kawaguchi, "The origins of two-state spontaneous membrane potential fluctuations of neostriatal spiny neurons," *J. Neurosci.*, vol. 16, no. 7, pp. 2397–2410, Apr. 1996. [Online]. Available: <http://www.jneurosci.org/content/16/7/2397.short>
- [134] E. A. Stern, D. Jaeger, and C. J. Wilson, "Membrane potential synchrony of simultaneously recorded striatal spiny neurons in vivo." *Nature*, vol. 394, no. 6692, pp. 475–8, Jul. 1998. [Online]. Available: <http://www.nature.com/nature/journal/v394/n6692/full/394475a0.html#B3>
- [135] F. Kasanetz, L. A. Riquelme, and M. G. Murer, "Disruption of the two-state membrane potential of striatal neurones during cortical desynchronisation in anaesthetised rats," *The Journal of Physiology*, vol. 543, no. 2, pp. 577–589, Sep. 2002. [Online]. Available: <http://doi.wiley.com/10.1113/jphysiol.2002.0024786>
- [136] J. Tepper and D. Plenz, "Microcircuits in the striatum: striatal cell types and their interaction," in *Microcircuits: The Interface between Neurons and Global Brain Function (Dahlem Workshop Reports)*. MIT Press, 2006. [Online]. Available: <http://garcia.rutgers.edu/Reprints.pdfs/Dahlem.preprint.doc.pdf>
- [137] A. E. Kincaid, T. Zheng, and C. J. Wilson, "Connectivity and Convergence of Single Corticostriatal Axons," *J. Neurosci.*, vol. 18, no. 12, pp. 4722–4731, Jun. 1998. [Online]. Available: <http://www.jneurosci.org/content/18/12/4722.full>
- [138] J. Bolam, H. Bergman, A. Graybiel, and M. Kimura, "Microcircuits, molecules and motivated behaviour: microcircuits in the striatum," *Microcircuits: The Interface . . .*, 2006. [Online]. Available: https://scholar.google.com/scholar?q=bolam+microcircuits+molecules&btnG=&hl=nl&as_sdt=0%2C5#3
- [139] S. Khurana and W.-K. Li, "Baptisms of fire or death knells for acute-slice physiology in the age of 'omics' and light?" *Reviews in the neurosciences*, vol. 24, no. 5, pp. 527–36, Jan. 2013. [Online]. Available: <http://www.degruyter.com/view/j/revneuro.2013.24.issue-5/revneuro-2013-0028/revneuro-2013-0028.xml>
- [140] B. R. Lee, P. Mu, D. B. Saal, C. Ulibarri, and Y. Dong, "Homeostatic recovery of downstate-upstate cycling in nucleus accumbens neurons." *Neuroscience letters*, vol. 434, no. 3, pp. 282–8, Apr. 2008. [Online]. Available: <http://www.pubmedcentral.nih.gov/articlerender.fcgi?artid=2366058&tool=pmcentrez&rendertype=abstract>
- [141] U. Frey, U. Egert, F. Heer, S. Hafizovic, and A. Hierlemann, "Microelectronic system for high-resolution mapping of extracellular electric fields applied to brain slices." *Biosensors & bioelectronics*, vol. 24, no. 7, pp. 2191–8, Mar. 2009. [Online]. Available: <http://www.sciencedirect.com/science/article/pii/S095656630800643X>
- [142] K. Deisseroth, "Optogenetics." *Nature methods*, vol. 8, no. 1, pp. 26–9, Jan. 2011. [Online]. Available: <http://dx.doi.org/10.1038/nmeth.f.324>
- [143] A. V. Kravitz, S. F. Owen, and A. C. Kreitzer, "Optogenetic identification of striatal projection neuron subtypes during in vivo recordings." *Brain research*, vol. 1511, pp. 21–32, May 2013. [Online]. Available: <http://www.pubmedcentral.nih.gov/articlerender.fcgi?artid=3594574&tool=pmcentrez&rendertype=abstract>
- [144] S. Zhao, J. T. Ting, H. E. Atallah, L. Qiu, J. Tan, B. Gloss, G. J. Augustine, K. Deisseroth, M. Luo, A. M. Graybiel, and G. Feng, "Cell typespecific channelrhodopsin-2 transgenic mice for optogenetic dissection of neural circuitry function," *Nature Methods*, vol. 8, no. 9, pp. 745–752, Aug. 2011. [Online]. Available: <http://dx.doi.org/10.1038/nmeth.1668>
- [145] Y. Buskila, P. P. Breen, J. Tapson, A. van Schaik, M. Barton, and J. W. Morley, "Extending the viability of acute brain slices." *Scientific reports*, vol. 4, p. 5309, Jan. 2014. [Online]. Available: <http://www.nature.com/srep/2014/140616/srep05309/full/srep05309.html>
- [146] S. Huang and M. Y. Uusisaari, "Physiological temperature during brain slicing enhances the quality of acute slice preparations." *Frontiers in cellular neuroscience*, vol. 7, p. 48, Jan. 2013. [Online]. Available: <http://www.pubmedcentral.nih.gov/articlerender.fcgi?artid=3632751&tool=pmcentrez&rendertype=abstract>

REFERENCES

- [147] A. Ivanov and Y. Zilberter, "Critical state of energy metabolism in brain slices: the principal role of oxygen delivery and energy substrates in shaping neuronal activity." *Frontiers in neuroenergetics*, vol. 3, p. 9, Jan. 2011. [Online]. Available: <http://www.pubmedcentral.nih.gov/articlerender.fcgi?artid=3247678&tool=pmcentrez&rendertype=abstract>
- [148] J. H. Ye, J. Zhang, C. Xiao, and J.-Q. Kong, "Patch-clamp studies in the CNS illustrate a simple new method for obtaining viable neurons in rat brain slices: glycerol replacement of NaCl protects CNS neurons." *Journal of neuroscience methods*, vol. 158, no. 2, pp. 251–9, Dec. 2006. [Online]. Available: <http://www.sciencedirect.com/science/article/pii/S0165027006002950>
- [149] D. G. MacGregor, M. Chesler, and M. E. Rice, "HEPES prevents edema in rat brain slices," *Neuroscience Letters*, vol. 303, no. 3, pp. 141–144, May 2001. [Online]. Available: <http://www.sciencedirect.com/science/article/pii/S0304394001016901>
- [150] Y. Pichon and J. E. Treherne, "Extraneuronal Potentials and Potassium Depolarization in Cockroach Giant Axons," *J. Exp. Biol.*, vol. 53, no. 2, pp. 485–493, Oct. 1970. [Online]. Available: <http://jeb.biologists.org/content/53/2/485.short>
- [151] T. Parittotokkaporn, J. Sirirattanapan, P. Yu, M.-C. Hsiao, D. Song, and T. W. Berger, "Focal potassium microinjection in rat hippocampal slices inducing interictal activities," in *The 4th 2011 Biomedical Engineering International Conference*. IEEE, Jan. 2012, pp. 269–272. [Online]. Available: <http://ieeexplore.ieee.org/lpdocs/epic03/wrapper.htm?arnumber=6172068>
- [152] D. Purves, G. J. Augustine, and D. Fitzpatrick, *Neuroscience, 4th Edition*, 2008.
- [153] J. Campbell, Neil; Reece, *Biology*. Benjamin Cummings Publishing Company, Inc, 1996.

Appendix A

Electrophysiological recording of neuronal signals

Standard textbooks of neurophysiology dictate that neurons communicate via connections called synapses [152]. The neuron's output is the axon, which connects to the input dendrites of another neuron. A neuron can have an intricate structure of branching dendrites, integrating inputs from multiple neurons via a large number of synapses. The most common synapse is the chemical synapse, as seen in figure A.1. When an action potential arrives, the presynaptic neuron releases neurotransmitter into the synaptic cleft, which binds to receptors on the postsynaptic neuron. Binding of such receptors will alter the behaviour of ion channels in the cell membrane, resulting in an effective in- or outflux of ions. This in turn leads to a concentration gradient and change in the transmembrane potential. This change is called an excitatory postsynaptic potential (EPSP) if it brings the neuron closer to its activation threshold, while a move away from the threshold is an inhibitory postsynaptic potential (IPSP). The structure of the chemical synapse results in unidirectional signalling. Bidirectional signalling is possible via electrical synapses (also called gap junctions), which are generally much faster but produce more simple behaviour than the chemical synapse.

A neuron integrates all EPSP's and IPSP's from its dendritic synapses and if this results in a threshold crossing, it will evoke an action potential. In this way, the organisation and structure of the dendrites can form a complex method for signal processing and information relay selection. This is a dynamic process, since neurons can adjust their connectivity as a result of previous input (this is called synaptic plasticity). Active connections are strengthened while inactive connections are abandoned in time, allowing for complex behaviour such as memory.

Neuronal activity can be measured in the extracellular space by measuring the electric field potential arising from the concentration gradients. Conversely, it is possible to evoke neural activity by imposing a potential, usually through the injection of current. In the extracellular space, neurons behave as current sources and sinks and can be linearly added. Electrodes close to a group of neurons can record activity from the entire ensemble. However, at larger distances from the neuronal activity, the capacitive low-pass nature of the extracellular space reduces high frequency components, effectively obscuring action potentials. Nevertheless, ensemble activity can be recorded as local field potentials (LFP) which reflect slower trends in neuronal activity and as such can be interpreted as a measure of synchrony in the neighbouring neurons. By applying filters to the recorded signals, it is possible to observe both single neuron spiking (high frequency) and ensemble activity (low frequency) from near neurons. This makes measurements of electrical potentials in the extracellular space a valuable and versatile tool for analysing neuronal functioning.

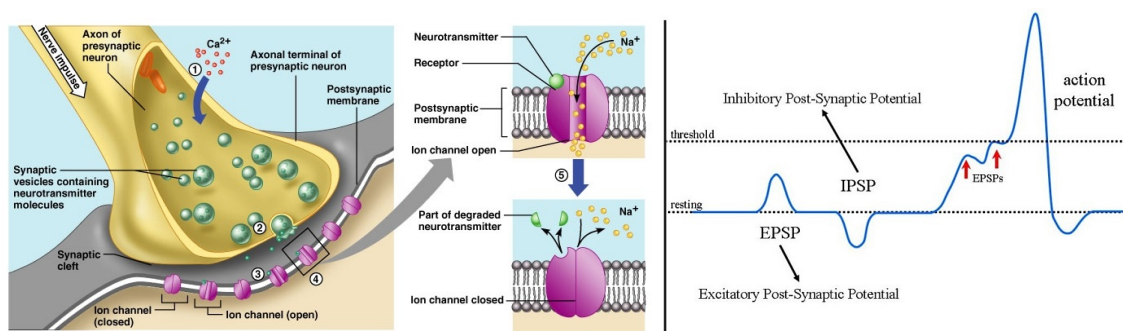


Figure A.1: *Left*: an excitatory chemical synapse, as presented in [153]. Neurotransmitter released by the presynaptic neuron will bind to receptors in the postsynaptic neuron, triggering channel opening. The resulting ion influx increases the postsynaptic potential. *Right*: Postsynaptic potentials will be summed up and if the threshold of the voltage-dependent gates is crossed, an action potential occurs.

Appendix B

Disregarded cluster templates

This is an overview of the 8 main cluster waveform shapes that were semi-manually discarded as noise. These clusters make up 71% of recorded clusters, after automatic elimination. Although most clusters show typical monophasic templates, several more distinct waveforms are shown. However, these waveforms are still contaminated with noise waveforms and as such still discarded.

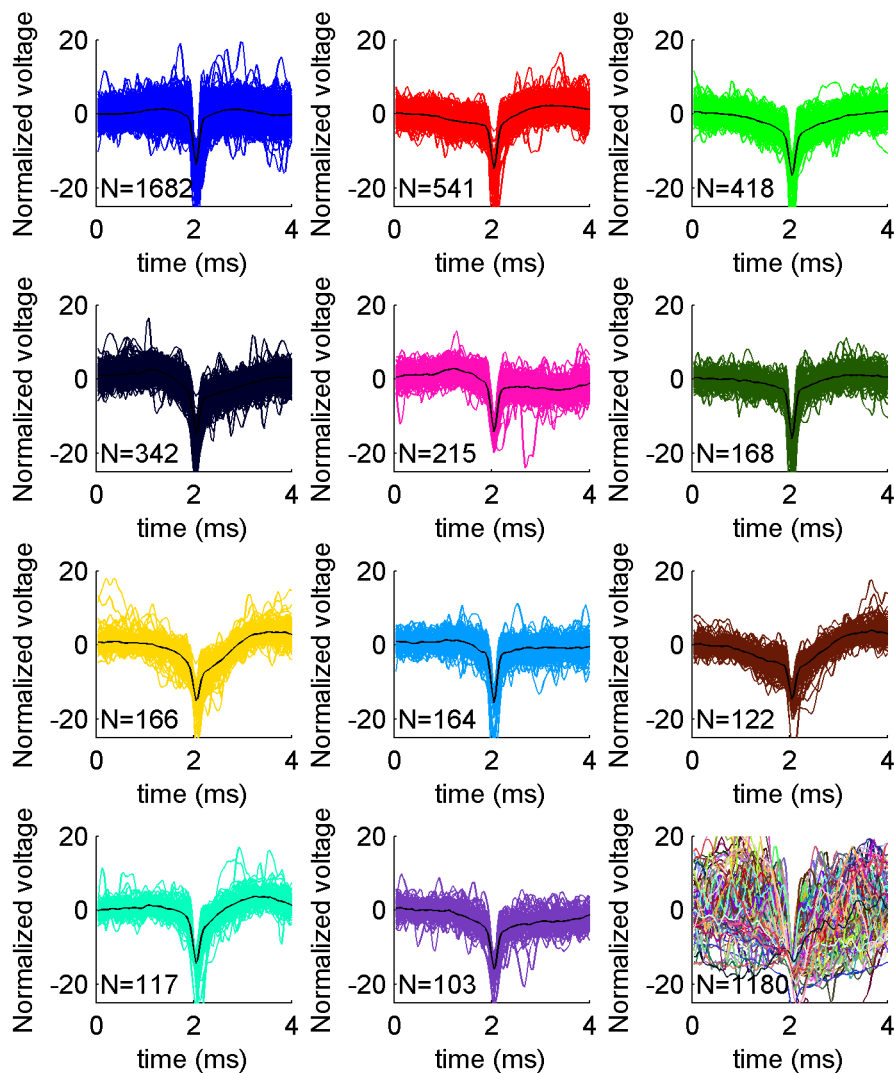


Figure B.1: Overview of noise waveforms, as clustered using PCA. The lower right plot shows mean waveforms for unclassified waveforms, which could not be clustered.

Appendix C

Local field potentials

To obtain LFP's, recordings of raw electrode data are first filtered by subtracting the mean, applying a low-pass filter (6th order butterworth filter, cutoff=100Hz) and a powerline filter (notch filter, 50Hz, Q=35). For each electrode, the spectrogram and periodogram are calculated. Signals are resampled at 250Hz and the spectrogram is calculated with a frequency resolution of 0.1Hz and a time resolution of 5s. The periodogram is calculated using the default matlab command.

Here an example of the results is shown, as recorded simultaneously with action potentials. This shows that although a burst of activity is seen, LFP signals do not reflect this. More work is required to understand if more meaningful information can be extracted from the LFP.

